1   **ENVIRONMENTALLY ASSOCIATED CHROMOSOMAL STRUCTURAL VARIATION**

2   **INFLUENCES FINE-SCALE POPULATION STRUCTURE OF ATLANTIC SALMON**

3   **(*Salmo salar*)**

4   **Running title:** Environmentally mediated chromosomal translocation

5

6   K. Beth Watson[1,2*], Sarah J. Lehnert[2], Paul Bentzen[1], Tony Kess[2], Antony Einfeldt[1], Steven

7   Duffy[2], Sigbjørn Lien[3], Matthew Kent[3], Ben Perriman[1], and Ian R. Bradbury[1,2]

8

9   1: Department of Biology, Dalhousie University, Halifax NS, Canada

10 2: Northwest Atlantic Fisheries Centre, Fisheries and Oceans Canada, St. John's NL, Canada

11 3: Centre for Integrative Genetics, Norwegian University of Life Sciences, Ås Norway

12

13 *Correspondence: Beth Watson, Department of Biology Life Sciences Centre, Dalhousie

14 University, 1355 Oxford Street, PO Box 15000, Halifax NS, Canada, B3H 4R2

15 Tel: +1 (902-494-1398)

16 Email: beth.watson@dal.ca

17

18

19

20

21

Abstract. Chromosomal rearrangements (e.g., inversions, fusions, and translocations) have long

been associated with environmental variation in wild populations. New genomic tools provide the

opportunity to examine the role of these structural variants in shaping adaptive differences within

and among wild populations of non-model organisms. In Atlantic Salmon (*Salmo salar*),

variations in chromosomal rearrangements exist across the species natural range, yet the role and

importance of these structural variants in maintaining adaptive differences among wild

populations remains poorly understood. We genotyped Atlantic Salmon ($n = 1429$) from 26

populations within a highly genetically structured region of southern Newfoundland, Canada with

a 220K SNP array. Multivariate analysis, across two independent years, consistently identified

variation in a structural variant (translocation between chromosomes Ssa01 and Ssa23),

previously associated with evidence of trans-Atlantic secondary contact, as the dominant factor

influencing population structure in the region. Redundancy analysis suggested that variation in

the Ssa01/Ssa23 chromosomal translocation is strongly correlated with temperature. Our analyses

suggest environmentally mediated selection acting on standing genetic variation in genomic

architecture introduced through secondary contact may underpin fine-scale local adaptation in

Placentia Bay, Newfoundland, Canada, a large and deep embayment, highlighting the importance

of chromosomal structural variation as a driver of contemporary adaptive divergence.

1 INTRODUCTION

Elucidating the genetic basis of adaptation is central to the understanding of evolutionary biology (Schluter, 2009). Adaptive differences, accumulated through selection imposed by spatially and temporally heterogenous environments, enable persistence (Felsenstein, 1976; Savolainen, Lascoux, & Merilä, 2013) and drive the diversification of life (Dobzhansky, 1951). Genome-scale data, now available for many non-model organisms, are highlighting the potential of genomic architecture to facilitate adaptive divergence (Campbell et al., 2018; Wellenreuther et al., 2019) with chromosomal structural variants (e.g., inversions, fusions, and translocations) increasingly being identified and associated with environmental and life history variation (see Wellenreuther & Bernatchez, 2018). However, understanding of (i) the origins of chromosomal structural variants (Rougemont & Bernatchez, 2018; Fuller, Koury, Phadnis, & Schaeffer, 2019; Marques, Meier, & SeeHausen, 2019), (ii) associations between structural variants and complex phenotypes (Lee et al., 2017; Fuller et al., 2019; Jay et al., 2019), and (iii) the effectiveness of different types of structural variants as drivers of adaptive divergence (Rieseberg, 2001; Guerrero & Kirkpatrick, 2014) remains limited.

Chromosomal structural variants can be caused by changes in copy number (insertion, deletion and duplication), orientation (inversion) or position (translocation and fusion). To date, most work has focused on inversion polymorphisms (Dobigny, Britton-Davidian, & Robinson, 2017) due to the potential for strong suppression of recombination and reduced fertility in heterozygous individuals (Sturtevant, 1917; White, 1978; King, 1993). Inversions are taxonomically widespread (Kirkpatrick & Barton, 2006; Wellenreuther & Bernatchez, 2018), frequently polymorphic within and between species and populations (Sturtevant, 1938; Dobzhansky, 1951; White, 1978), and commonly align with environmental gradients (Balanyà,

68   Huey, Gilchrist, & Serra, 2009; Kennington & Hoffmann, 2013; Kapun, Fabian, Goudet, & Flatt,

69   2016), or complex morphological and behavioural phenotypes (Huang, Andrew, Owens, Ostevik,

70   & Rieseberg, 2019; Sinclair-Waters et al., 2018). Unlike inversions that change gene order

71   (Fuller et al., 2019), translocations and fusions physically unlink or link genes and reduce

72   recombination within each newly linked chromosome arm (Dumas & Britton-Davidian, 2002)

73   reducing recombination in both heterozygotes and rearranged homozygotes (Bidau, Giménez,

74   Palmer, & Searle, 2001; Castiglia & Capanna, 2002). The potential of translocations and fusions

75   to facilitate adaptation (Charlesworth, 1985) is supported by recent theoretical modeling work

76   (Guerrero & Kirkpatrick, 2014), and empirical evidence of environmental correlations with

77   fusions and translocations (*Drosophila americana*, McAllister, 2003; *Dichroplus sp.*, Bidau,

78   Miño, Castillo, & Martí, 2012; Atlantic Salmon, Wellband et al., 2019). However, translocations

79   and fusions remain understudied with little reporting of the distribution or frequency of

80   polymorphisms, and associated phenotypic and environmental variation (Dobigny et al., 2017).

81   Atlantic Salmon (*Salmo salar*) span the North Atlantic Ocean exhibiting hierarchical

82   spatial structure across their range (King et al., 2007). Genomic differentiation is greatest

83   between continents with eastern (European) and western (North American) populations having

84   diverged more than 600,000 years before present (bp) (Nilsson et al., 2001; King et al., 2007;

85   Rougemont & Bernatchez, 2018). Over the intervening period numerous differences have

86   accumulated including large chromosomal rearrangements, two fusions (Ssa08/Ssa29 and

87   Ssa26/Ssa28) and a translocation (Ssa01/Ssa23) (Brenna-Hansen et al., 2012; Wellband et al.,

88   2019; Lehnert et al., 2019a), which have reduced the number of chromosome pairs from 29 in

89   Europe to 27 in North America (Hartley, 1988; Phillips & Ráb, 2001). Recent findings suggest

90   that variation in the Ssa01/Ssa23 chromosomal translocation exists in North America, and that

91   this variation was likely introduced through trans-Atlantic secondary contact from European

92   Atlantic Salmon near the end of the last glacial maximum (LGM) approximately 18,000 bp

93   (Bradbury et al., 2015; Rougemont & Bernatchez, 2018). Lehnert et al. (2019a) found that the

94   frequency of the Ssa01/Ssa23 translocation changed with latitude across Atlantic Canada with

95   more northern locations, such as sites in Newfoundland and Labrador, exhibiting the highest

96   frequency of the European karyotype (no Ssa01/Ssa23 translocation) relative to southern

97   populations which were almost entirely fixed for the North American karyotype (Ssa01/Ssa23

98   translocation). The importance of this structural variation resulting from secondary contact, and

99   the mechanisms acting to maintain high levels of polymorphism within and across Atlantic

100   Salmon populations in Atlantic Canada remain unknown.

101   Here we explore fine-scale spatial variation in southern Newfoundland, Canada, an area

102   with pronounced regional spatial structure (Bradbury et al., 2014), and evidence of trans-Atlantic

103   secondary contact (King et al., 2007; Bradbury et al., 2015). We first examine genomic variation

104   within Atlantic Salmon among 26 rivers using two discrete years of sampling and identify

105   variation in the Ssa01/Ssa23 translocation as a major driver of population structure. We examine

106   temporal stability of population structure as well as the frequency of this structural variation

107   within and among rivers. Next, we identify environmental associations with population structure

108   and consequently the Ssa01/Ssa23 translocation. We build directly on previous work that

109   identified range-wide polymorphism of a translocation between chromosomes Ssa01 and Ssa23

110   across Atlantic Canada (Lehnert et al., 2019a) and mitochondrial DNA evidence of trans-Atlantic

111   secondary contact along southeastern Newfoundland (King et al., 2007; Bradbury et al., 2015)

112   and highlight the potential role of chromosomal structural variation in fine-scale local adaptation

113 and the importance of secondary contact in generating standing genetic variation and driving

114 contemporary adaptive divergence.

115

116 **2 METHODS**

117 **2.1 Sampling and genotyping**

118 Juvenile Atlantic Salmon, young-of-the-year (YOY) and parr (ages 0 to 2+), were

119 collected by electrofishing during the period July to September of 2017 and 2018 from 26 rivers

120 around Placentia Bay, a large (145 km wide at the mouth by 125 km long), deep bay (240 m)

121 separating the Avalon and Burin Peninsulas on the south coast of Newfoundland, Canada (Figure

122 1 and Table 1). Two rivers, Lance (LAN) and Little Barasway (LBB), were excluded from

123 sampling in 2018 due to small sample size in 2017. Cohorts were assigned based on age-length

124 relationships validated by scale ageing (Sylvester et al., 2019). Fin clips were collected and

125 preserved in 95% ethanol. DNA was extracted using DNeasy Blood and Tissue or DNeasy 96

126 Blood and Tissue kits (Qiagen, Toronto, ON, Canada) following manufacturer's protocols.

127 Concentration of extracted DNA was assessed using a Nanodrop spectrophotometer and by

128 agarose gel visualization. DNA was standardized to a concentration of 15 ng/µl. A total of 1429

129 (2017: 745 and 2018: 684) individuals were genotyped by Centre for Integrative Genetics

130 (CIGENE, Ås, Norway) using a 220K bi-allelic single nucleotide polymorphism (SNP)

131 Affymetrix Axiom array developed for Atlantic Salmon as described in Barson et al. (2015).

132 These SNPs were a subset of those in the 930K XHD *Ssa*l array (dbSNP accession numbers

133 ss1867919552–ss1868858426) designed using Norwegian aquaculture salmon. Genotype data

134 were filtered for high quality SNPs based on their clustering patterns and subsequent filtering was

135 performed using PLINK v 1.9 (Purcell et al., 2007; Chang et al., 2015). SNPs were filtered for a

136   minor allele frequency (MAF) cut-off of 0.01, a missingness threshold of 0.05 across samples,

137   and non-biallelic loci within each year sampled. SNPs were retained only if they passed filtering

138   in both years resulting in a total of 139,038 SNPs. In addition, samples were filtered to retain

139   only individuals with <5% missing genotypes, resulting in a total of 662 and 611 individuals in

140   2017 and 2018, respectively.

141

142   **2.2 Detection of population structure**

143   For population genetic analyses that require a panel of neutral and unlinked loci we first

144   used PLINK version 1.9 (Chang et al., 2015) to identify outlier loci (F_{ST} > 95th percentile) among

145   sample sites. Loci identified as outliers in both 2017 and 2018 were removed. We then removed

146   SNPs with high physical linkage using a sliding-window approach in PLINK version 1.9. SNPs

147   with a variance inflation factor (VIF) greater than 2 were removed from 50 SNP windows shifted

148   by five SNPs each iteration. We further removed all SNPs on chromosomes with known

149   structural variants Ssa01/Ssa23 and Ssa08/Ssa29 (Lehnert et al., 2019a). This neutral, unlinked

150   dataset was then thinned, keeping one SNP per 200,000 bases, using PLINK version 1.9 (Chang et

151   al., 2015).

152   Indices of genetic diversity including observed and expected heterozygosity (H_o and H_e)

153   and F_{IS} (Nei, 1987), were calculated per river and year to assess deviation from Hardy-Weinberg

154   equilibrium. Indices were calculated using the *basic.stats* function in the R package *hierfstat*

155   (Goudet, 2005) with the neutral, unlinked dataset (n = 6,302 SNPs). Confidence intervals for

156   river-specific F_{IS} were calculated using the *boot.ppfis* function in *hierfstat* (Goudet, 2005) with

157   1,000 bootstrap replicates. Genetic differentiation was assessed by calculating pairwise F_{ST} (Weir

158   and Cockerham, 1984) between rivers using the *stamp.fst* function, with 100 bootstrap replicates,

159   in the R package *StAMPP* (Pembleton, Cogan, & Forster, 2013) and visualized using *gplots*

160   (Warnes et al., 2016).

161   To estimate the number of distinct genetic clusters in each year, ADMIXTURE version 1.3

162   (Alexander, Novembre & Lange, 2009), which calculates individual ancestry proportions using

163   maximum likelihood estimates in a parametric model, was run for K (genetic clusters) 1 to 27

164   with three different random number seeds with the neutral, unlinked dataset (n = 6,302 SNPs).

165   From ADMIXTURE runs, standard deviation of cross-validation (CV) error was used to select a

166   reasonable range of K as in McCartney-Melstad, Vu & Shaffer (2018). Bar plots of estimated

167   individual ancestry proportions given by the Q-values were generated using R version 3.6.1 (R

168   Core Team, 2019).

169   The R package *pcadapt* (Luu et al., 2017) was then used to detect genomic regions

170   associated with population-based differences in genomic architecture across all 26 rivers in each

171   year. Multiple values of K (number of principal components; PCs), ranging from 1 to 100, were

172   explored. The R package *qvalue* (Storey et al., 2015) was used to correct for false-discovery rate

173   by transforming p-values for all SNPs into q-values which were plotted using the Manhattan plot

174   function in the R package *qqman* (Turner, 2014). The final number of PC axes retained was K =

175   2, as we were primarily interested in large scale patterns of population differentiation. The

176   inclusion of additional values of K highlighted inter-individual differences rather than population

177   level differences. Further, upon visual inspection of the Manhattan plots, we found that two

178   strongly divergent genomic regions localized on chromosomes Ssa01 and Ssa23, a known

179   chromosomal translocation (Brenna-Hansen et al., 2012; Lehnert et al., 2019a), were the

180   dominant source of variation across multiple values of K (see Results). These regions associated

181   with the chromosomal translocation were important drivers of differentiation along the first PC

182   axis and were thus a primary focus of our study. We note that physical genomic positions

183   presented in our study are based on the European Atlantic Salmon genome, where Ssa01 and

184   Ssa23 are separate chromosomes (Lien et al., 2016), which differs from the standard North

185   American karyotype where the p arm of Ssa01 has fused to Ssa23 (Brenna-Hansen et al., 2012).

186

187   **2.3 Environmental association analysis**

188   Spatial patterns of association between genomic variation and climatic (i.e., temperature

189   and precipitation) and habitat (i.e., axial river length, basin relief, number of obstructions, and

190   human population density) variables were investigated using partial redundancy analysis (RDA)

191   as implemented in the R package *vegan* (Oksanen et al., 2017). Environmental variables were

192   collected from publicly available sources (see Table S1). GPS coordinates of sample sites were

193   used to extract 19 BIOCLIM variables, interpolated monthly climate data at a spatial resolution of

194   30 arc-seconds averaged for the years 1970 – 2000, from the WorldClim 2.0 database (Fick &

195   Hijmans, 2017). Human population density, a proxy for habitat disturbance, was calculated as in

196   Lehnert et al. (2019b). Axial river length, number of obstructions, and basin relief were obtained

197   from Porter et al. (1974). Axial river length and number of obstructions were approximated using

198   GOOGLE EARTH and maximum elevation from HydroSHEDS digital elevation model (Lehner,

199   Verdin, & Jarvis, 2008) was substituted for basin relief for missing sites (Fair Haven Brook, Red

200   Harbour East, and Piercey's Brook). All climatic and habitat data were standardized using the

201   scale function in R (R Core Team, 2019).

202   Given that many of the climatic variables were highly correlated (r > 0.8), we first

203   performed a variable reduction step using PCA to summarize climatic variation, for temperature

204   and precipitation. The first two PCs of each PCA were retained to reduce dimensionality and

205   covariance of loadings. Next, latitude and longitude of each river mouth were determined using

206   GOOGLE EARTH. Geographic distance between each river mouth was calculated using the least-

207   cost distance function, constrained to a maximum depth of 100 m below sea-level, in the R

208   package *marmap* (Pante & Simon-Bouhet, 2013). Multivariate associations between genomic and

209   environmental data were tested using redundancy analysis (RDA), conditioned on geographic

210   distance from the most easterly site (Branch River), with four climatic summary variables (i.e.

211   PC1 and PC2 temperature, and PC1 and PC2 precipitation) and four habitat variables (i.e. basin

212   relief, number of obstructions, axial river length, and human population density) as predictors and

213   individual genotypes as dependent variables. Variance inflation factors were below 5 for all

214   variables indicating no multicollinearity between predictors. The RDA was visualized using the

215   plot function in R version 3.6.1 (R Core Team, 2019). The final number of RDA axes retained (n

216   = 3) was determined by visual inspection of the scree plot. To identify SNPs influenced by

217   climatic and habitat variation, we scaled and centred the raw scores on each constrained RDA

218   axis. We then identified outlier SNPs based on the loadings on each RDA axes, defined here as

219   SNPs more than three standard deviations from the mean. The Manhattan plot function in the R

220   package *ggman* (Rajagopal, 2020) was used to visualize each of the three retained RDA axes.

221   Visual inspection of the first RDA axis identified outlier SNPs localized on chromosomes Ssa01

222   and Ssa23, a known chromosomal translocation (Brenna-Hansen et al., 2012; Lehnert et al.,

223   2019a). The correlation between frequency of the Ssa01/Ssa23 chromosomal translocation and

224   environmental variation was further explored in subsequent analyses.

225

226   **2.4 Assignment of translocation karyotype**

227   Variation in the Ssa01/Ssa23 chromosomal translocation was found to be both a major

228   source of population level differentiation and associated with environmental variation. Therefore,

229   we next examined variation in translocation frequency. Using the results of *pcadapt*, outlier SNPs

230   (q-value < 0.05 in both 2017 and 2018, n = 887) in the outlier block regions, Ssa01 (44,000,000 -

231   53,000,000 bp) and Ssa23 (0 - 9,500,000 bp), were combined as in Lehnert et al. (2019a). Spatial

232   genetic structure of the Ssa01/Ssa23 chromosomal translocation was explored with principal

233   component analyses (PCA) performed using the R package *pcadapt* (Luu et al., 2017) with K = 3.

234   Based on clustering patterns on the first PC axis, on which individuals were separated into three

235   clusters consistent with Lehnert et al. (2019a), individuals were assigned a karyotype using the

236   kmeans function in R version 3.6.1 (R Core Team, 2019). The three clusters corresponded to

237   three karyotypes: 1) standard North American (homozygous translocated; Ssa01p/Ssa23 and

238   Ssa01q), 2) standard European (homozygous non-translocated; Ssa01p/q and Ssa23), and 3)

239   heterozygous (carrying a translocated and non-translocated copy of the chromosomes).

240   Karyotype assignment followed Lehnert et al. (2019a), which incorporated European samples;

241   greater genetic variation was observed on PC1 and PC2 for the standard European karyotype

242   relative to the standard North American karyotype. This pattern of variation in genetic diversity

243   was consistent in our analysis (see Results). Using these genotype assignments, genetic

244   differentiation (observed heterozygosity) between karyotypes was assessed by calculating

245   pairwise F_{ST} (Weir and Cockerham, 1984) between groups in PLINK version 1.9 (Chang et al.,

246   2015).

247   Neighbor-joining (NJ) trees based on Nei's D (Nei, 1972) were generated using outlier

248   loci (q-value < 0.05) within the outlier block regions on Ssa01 and Ssa23 and the R package

249   *StAMPP* (Pembleton et al., 2013). Trees were visualized using FIGTREE v1.4 (Rambaut, 2012).

250   Linkage disequilibrium (LD) was calculated among outlier SNPs ($q < 0.05$) on chromosomes

251   Ssa01 and Ssa23 between karyotypes. Pairwise LD (R^2) values were calculated using PLINK v 1.9

252   (Chang et al., 2015) and visualized using the R package *gplots* (Warnes et al., 2016).

253

254   **2.5 Frequency of translocation karyotype**

255   *Population variation and temporal stability*

256   Heterogeneity in translocation and karyotype frequencies between rivers was tested for

257   each year sampled (2017 and 2018) using an analysis of deviance in a generalized linear model

258   (GLM) with a binomial logistic transformation, followed by a comparison of contrasts as in

259   Mérot et al. (2018), and a pairwise Fisher's exact test adjusted for multiple comparisons.

260   Temporal stability of translocation and karyotype frequency within each river between years was

261   then tested using a pairwise Fisher's exact test. Two rivers, Lance (LAN), and Little Barasway

262   (LBB), were excluded from analysis due to limited sample size. To calculate translocation

263   frequency, we used the equation:

264   ((# homozygous translocated x 2) + (# heterozygotes)) / (# total individuals x 2)

265   which provides the frequency of the standard North American allele per river.

266

267   *Environmental associations*

268   Given the association between the Ssa01/Ssa23 chromosomal translocation and

269   environmental variables (see RDA above), we next tested for significant correlations between the

270   identified climatic variables (temperature and precipitation) and translocation frequency using

271   linear regression. In the model, the response variable was the frequency of the North American

272 allele (Ssa01p/Ssa23) or the standard North American karyotype (homozygous translocated) and

273 the explanatory variable being the climatic summary variables (see Results).

274

275 **2.6 Gene ontology**

276   We examined functional enrichment of genes associated with the Ssa01/Ssa23

277 chromosomal translocation and identified as significant environmental outliers ($q < 0.05$) on

278 RDA1. We conducted gene ontology (GO) enrichment analysis using GO annotations in the

279 Atlantic Salmon genome from SalmoBase (Samy et al., 2020). A reference set of genes, genes

280 within 10 kb of all 138,451 SNPs from the array, was identified and extracted using BEDTOOLS

281 (Quinlan & Hall, 2010). Outlier sets of genes, genes within 10 Kb of outlier SNPs on RDA1 and

282 located within the translocation were then extracted for 2017 ($n = 914$) and 2018 ($n = 700$). The

283 R package *topGO* version 2.38.1 (Alexa, Rahnenführer, & Lengauer, 2006) was then used to test

284 for over-representation of GO biological processes using a node size of 5 and the 'weight01'

285 algorithm to account for structural relationships among GO terms. An alpha level of 0.01 was

286 used to determine significance. Using the same outlier sets of genes we then tested for

287 enrichment of gene profiles using the R package CLUSTERPROFILER (Yu, Wang, Han, & He,

288 2012). NCBI gene ID numbers were used as search criteria in the Kyoto Encyclopedia of Genes

289 and Genomes (KEGG) (Kanehisa, Goto, Sato, Furumichi, & Tanabe, 2012). An alpha level of

290 0.01 was used to determine significance.

291

292 **3 RESULTS**

293 **3.1 Sampling and genotyping**

294   In total, 662 individuals sampled in 2017 and 611 individuals sampled in 2018 were

295 genotyped and passed quality control thresholds. Exploratory analysis using principal component

296 analysis (PCA) found genetic variation separated Red Harbour East (RHA) from all other rivers

297 along the first two principal component (PC) axes in both 2017 and 2018 (Figure S1). Due to the

298 prevalence of non-anadromous Atlantic Salmon along the south coast of Newfoundland

299 (Verspoor, McGinnity, Bradbury, & Glebe, 2015) and the verification of a significant waterfall at

300 the mouth of RHA, this river was excluded following analyses of neutral genetic structure as

301 these individuals most likely represent a highly divergent landlocked population. A total of

302 138,451 SNPs, with a high overall genotyping rate (> 99%), and 632 individuals in 2017 and 585

303 individuals in 2018 were used in downstream analyses.

304

305 **3.2 Detection of population structure**

306   All rivers exhibited significant genetic differentiation ($p < 0$). Patterns of pairwise F_{ST}

307 clearly indicated strong regional structure within Placentia Bay consistent across both discrete

308 years sampled (Figure S2). Pairwise F_{ST}, which ranged from 0.0062 to 0.11 in 2017 and 0.0077

309 to 0.083 in 2018, was greatest between rivers along the Burin (Bay de l'Eau (BDL) – Piercey's

310 Brook (PBR)) and Avalon (Branch (BRA) – Ship Harbour (SHI)) Peninsulas indicative of an

311 east-west divide. Rivers along the Avalon Peninsula exhibited a higher degree of genetic

312 differentiation relative to each other as compared to rivers along the Burin Peninsula or head of

313 the bay where neighboring rivers exhibited little genetic differentiation. Interestingly, Cuslett

314 River (CUS) was found to be genetically similar to more geographically distant rivers along the

315 Burin Peninsula than neighboring rivers on the Avalon Peninsula. Observed (H_o) and expected

316 (H_e) heterozygosity ranged from 0.16 to 0.20 (mean = 0.19) in both 2017 and 2018. Inbreeding

317   coefficient (F_{IS}) ranged from -0.067 to -0.018 (mean = -0.026) in 2017 and -0.036 to 0.00 (mean

318   = -0.023) in 2018 (Table 2).

319   Fine-scale population structure was observed using a panel of putatively neutral loci

320   (6,302 SNPs with F_{ST} < 0.05 globally in both 2017 and 2018; known chromosomal

321   rearrangements excluded). The value of K with the lowest mean CV error in ADMIXTURE was K =

322   11 in 2017, and K = 9 in 2018. The reasonable range of K, values that had standard deviations

323   that overlapped with the lowest mean CV error were K = 10 and 12 – 14 in 2017, and K = 10 – 11

324   in 2018 (Figure S3). Red Harbour East (RHA) appeared distinct across all values of K in both

325   years sampled. Although the majority of rivers formed river-specific clusters in both years

326   sampled, the head of the bay (CBC – SHA) appeared to form an admixed cluster, most similar to

327   rivers along southern Burin Peninsula, across all values of K in both 2017 and 2018 (Figure S4).

328   We also explored spatial structure within Placentia Bay by performing a principal

329   component analysis (PCA) on the full data set (n = 138,451 SNPs). This analysis similarly found

330   genetic variation separated populations by geographic region along the first two PC axes, with

331   PC1 (variance explained in 2017: 1.8% and 2018: 2.4%) highlighting an east-west divide within

332   Placentia Bay and PC2 (variance explained in 2017: 1.2% and 2018: 1.6%) a north-south divide

333   along the Avalon Peninsula (Figure 2a, b). This pattern of spatial structure was found to be

334   temporally stable with the exception of Northwest Mortier Bay (NMB), which in 2017 clustered

335   more closely with the Avalon Peninsula than the Burin Peninsula on which it is located.

336   Divergence among clusters identified by PC1 was found to be driven by large outlier block

337   regions (> 8 Mbp; Table S2) on both chromosomes Ssa01 and Ssa23 (Figure 2c, d). Each peak of

338   genetic differentiation (Ssa01 and Ssa23) contained > 400 SNPs that were statistical outliers (q <

339   0.05) in both years. An increasing number of PC axes tested (K = 2 – 100; see Supplementary

340   Information Figure S5) supported Ssa01 and Ssa23 as the dominant factor driving genomic

341   divergence among Atlantic Salmon within Placentia Bay. In a range-wide study, Lehnert et al.

342   (2019a) found genomic divergence driven by Ssa01 and Ssa23 indicative of polymorphism in a

343   known chromosomal translocation that differentiates European and North American salmon

344   (Brenna-Hansen et al., 2012). As in Lehnert et al., (2019a), outlier block regions on Ssa01 and

345   Ssa23 were combined and analyzed together in downstream analyses (see below).

346

347   **3.3 Environmental association analysis**

348   PCA-based reduction of climatic variables was used to construct summary variables for

349   temperature and precipitation. For the PCA of temperature variables, the first PC axis explained

350   47.1% of site environmental variation and was positively associated with temperature seasonality

351   (BIO4) and temperature annual range (BIO7) but negatively associated with minimum

352   temperature of the coldest month (BIO 6), while the second PC axis explained 2.0% of site

353   environmental variation was most strongly negatively associated with annual mean temperature

354   (BIO1) (Table S3). For the PCA of precipitation variables, the first PC axis of the summary

355   variable for precipitation explained 65.1% of site environmental variation and was most strongly

356   negatively associated with annual precipitation (BIO12), while the second PC axis explained

357   2.3% of site environmental variation and was strongly positively associated with precipitation

358   seasonality (BIO15).

359   In the RDA, total proportion of genetic variance explained by the constraining

360   (environmental) variables was 4.3% and 4.4% with 0.85% and 1.3% of the total proportion of

361   variance explained by the conditioning variable (distance from the most easterly site; BRA) in

362   2017 and 2018 respectively. We found temperature and precipitation explained the greatest

363   proportion of genetic variance on RDA1 based on vector length and number of significant SNPs.

364   A total of 422 and 222 SNPs were significantly associated with temperature PC1 and 114 and

365   440 SNPs were significantly associated with precipitation PC1 on RDA1 in 2017 and 2018

366   respectively. In both discrete years sampled, SNP loadings on RDA1 indicated a strong

367   association with the Ssa01/Ssa23 outlier block regions previously identified (Figure 3c, d),

368   suggesting an association between the translocation and environmental variation. Genetic

369   variance associated with temperature was most strongly driven by rivers at the head of Placentia

370   Bay and along the Burin Peninsula (Figure 3a, b), a pattern that was consistent across years.

371   Whereas genetic variance associated with precipitation was most strongly driven by rivers along

372   southern Burin and Avalon Peninsulas (Figure 3a, b).

373

374   **3.4 Assignment of translocation karyotype**

375   Given that variation in the Ssa01/Ssa23 chromosomal translocation was identified as a

376   major source of genetic structure, and found to be associated with environmental variation, we

377   next examined translocation and karyotype frequency. Analysis of outlier SNPs ($n = 887$) within

378   the outlier block regions on Ssa01/Ssa23 found three distinct clusters on PC1 (variance explained

379   in 2017: 54.3% and 2018: 53.6%) (Figure 4a, b), consistent with a chromosomal rearrangement.

380   Similar clustering patterns were found using neighbor-joining (NJ) trees (Figure 4c, d).

381   Karyotype was assigned to each of the three clusters (based on PCA) with individuals assigned as

382   either: 1) standard North American (homozygous translocated; Ssa01p/Ssa23 and Ssa01q), 2)

383   standard European (homozygous non-translocated; Ssa01p/q and Ssa23), and 3) heterozygous

384   (carrying a translocated and non-translocated copy of the chromosomes). The heterokaryotype

385   was found to be intermediate to the homokaryotypes along PC1 (Figure 4). Individuals from

386   throughout Placentia Bay were found in each of the three clusters suggesting karyotype clusters

387   were not completely driven by the geography of the bay. Interestingly, the cluster of individuals

388   found to have the standard European karyotype (homozygous non-translocated; Ssa01p/q and

389   Ssa23) exhibited greater genetic variation along the first two PC axes than the clusters of

390   heterozygous or standard North American karyotype (homozygous translocated; (Ssa01p/Ssa23

391   and Ssa01q) individuals which exhibited the least amount of genetic variation along the first two

392   PC axes (Figure 4a, b).

393   Genetic differentiation (F_{ST}) between homokaryotypes was significantly greater ($p < 0.001$)

394   within the Ssa01/Ssa23 outlier block regions (Ssa01: $F_{ST} = 0.55$ and $F_{ST} = 0.52$, and Ssa23: $F_{ST} =$

395   0.71 and $F_{ST} = 0.70$ in 2017 and 2018 respectively) relative to that observed genome wide ($F_{ST} =$

396   0. 0094 and $F_{ST} = 0. 0096$ in 2017 and 2018 respectively). Heatmaps of linkage disequilibrium

397   (LD) between outlier SNPs ($q < 0.05$) on chromosomes Ssa01 and Ssa23 revealed regions of high

398   LD, in all pairwise comparisons of translocation karyotype (Figure S6). As expected, linkage

399   disequilibrium (R^2) was highest between homokaryotypes. Interestingly, LD between the

400   heterokaryotype and standard European karyotype was found to be lower than that observed

401   between the heterokaryotype and standard North American karyotype. Heterozygosity was found

402   to be four times higher for the standard European karyotype relative to the standard North

403   American karyotype within the outlier block regions (Figure S7).

404

405   **3.5 Frequency of translocation karyotype**

406   ***Population variation and temporal stability***

407   All rivers were polymorphic for the Ssa01 and Ssa23 chromosomal translocation (Figure

408   S8). Frequency of the translocation did not significantly differ between years ($p = 0.263$) but did

409   differ significantly between rivers within years ($p < 0.01$) (Figure S9). Average translocation

410   frequency (standard North American 'allele') was 61.3% (range: 5.5 – 86.0%) in 2017 and 59.6%

411   (range: 6.7 – 94.5%) in 2018. Frequency of the standard North American karyotype (homozygous

412   translocated; Ssa01p/Ssa23 and Ssa01q) was 41.9% (range: 0 – 72.0%) in 2017 and 41.0%

413   (range: 0 – 89.9%) in 2018 (Table S4). Frequency of the translocation was temporally stable

414   within rivers across the two discrete years sampled with the exception of Northwest Mortier Bay

415   (NMB), Cuslett (CUS), and Big Salmonier (BSA) which differed significantly in both karyotype

416   and translocation frequency between 2017 and 2018 (Table S5). Translocation frequency

417   significantly increased in NMB and significantly decreased in CUS and BSA from 2017 to 2018

418   (Figure S10).

419

420   ***Environmental associations***

421   The translocation appeared spatially distributed along a longitudinal gradient with the

422   highest frequency of the standard North American karyotype found along central Burin Peninsula

423   and the head of Placentia Bay, and absent or occurring at low frequency along the Avalon

424   Peninsula (Figure 5). A pronounced transition in frequency of the translocation homokaryotype,

425   consistent across both years sampled, was observed between Ship Harbour Brook (SHI) and Fair

426   Haven Brook (FHB). SHI and FHB had an average of 2.3% and 42.7% standard North American

427   karyotype (homozygous translocated) individuals across years, respectively, suggesting an

428   increase in European ancestry (in this genomic region) between sites. Interestingly, variation in

429   translocation frequency between rivers was significantly correlated with temperature PC1 (2017:

430    $p = 0.067$ and 2018: $p = 0.0087$) (Figure 6) but not precipitation PC1 (Figure S11). The

431   translocation (standard North American allele) occurred more frequently in rivers that have a

432   lower minimum temperature in the coldest month and exhibited greater variability in temperature

433   both seasonally and annually.

434

435   **3.6 Gene Ontology**

436   We searched the *Salmo salar* genome for annotated genes within 10kb on either side of

437   each SNP within the outlier block regions on Ssa01 and Ssa23 identified as an environmentally

438   associated outlier on RDA1. We identified 260 and 241 unique genes in proximity to the 914 and

439   700 SNPs identified as RDA1 outliers within the Ssa01/Ssa23 chromosomal translocation in

440   2017 and 2018 respectively. These genes represent putative targets of selection. We found

441   functional enrichment of 26 and 35 gene ontology (GO) biological processes ($p < 0.01$, Table S6)

442   in 2017 and 2018 respectively. Of these, 21 GO biological processes were significantly enriched

443   ($p < 0.01$) in both 2017 and 2018. Of particular interest were processes related to immunity,

444   growth, and oxidative stress. Further, using the outlier SNPs identified above, enrichment tests in

445   KEGG indicated over-representation of the insulin signaling pathway in both 2017 ($p = 0.00763$)

446   and 2018 ($p = 0.00439$).

447

448   **4 DISCUSSION**

449   Chromosomal structural variation is a significant, yet poorly understood source of genetic

450   variation (Wellenreuther et al., 2019) which may underpin complex phenotype and life history

451   variation across a wide range of taxa (Dobigny et al., 2017). In contrast with chromosomal

452   inversions, which have been increasingly associated with adaptive variation (Lamichhaney et al.,

453   2016; Jay et al., 2018; Huang et al., 2019), few well-documented occurrences of fusion or

454   translocation polymorphisms in wild populations have been reported (see Bidau & Martí, 2002;

455　Dobigny et al., 2017; Wellband et al., 2019; Cayuela et al., 2020). Our study is among the first to

456　report evidence of an adaptive chromosomal translocation influencing spatial structure in the

457　wild. We found the Ssa01/Ssa23 chromosomal translocation, previously found to reflect trans-

458　Atlantic differences and secondary contact (Brenna-Hansen et al., 2012; Lehnert et al., 2019a), to

459　be polymorphic and associated with fine-scale spatial structure of Atlantic Salmon in Placentia

460　Bay, Newfoundland, Canada. Moreover, we found translocation frequency is significantly

461　correlated with environmental variation in the region. This work extends previous analyses

462　(Bradbury et al., 2015; Lehnert et al., 2019a) providing a high-resolution examination of trans-

463　Atlantic secondary contact in Atlantic Salmon in southern Newfoundland, and highlights the

464　importance of secondary contact, introgression, and chromosomal structural variation as drivers

465　of adaptive divergence.

466

467　**4.1 Chromosomal translocation drives fine-scale spatial structure**

468　　　In our study, Atlantic Salmon populations exhibited hierarchical spatial genetic structure

469　within Placentia Bay, with the greatest genetic differentiation occurring between the Avalon and

470　Burin Peninsulas. This is consistent with previous work by Bradbury et al. (2015) which

471　identified two discrete genetic clusters along southern Newfoundland, east and west, with a

472　boundary near the Burin Peninsula. Trans-Atlantic secondary contact has been suggested to be a

473　significant factor structuring this region. Gene flow following secondary contact has been

474　documented for many temperate species that experienced periods of range expansion and

475　contraction throughout the Quaternary (Hewitt, 2000; Tigano & Friesen, 2016). In Atlantic

476　Salmon, secondary contact between European and North American salmon occurred, most

477　recently, during the Pleistocene at the end of the last glacial maximum (King et al., 2007;

478   Rougemont & Bernatchez, 2018) and is supported by evidence of European mitochondrial DNA

479   (King et al., 2007; Bradbury et al., 2015), and recently the identification of a chromosomal

480   polymorphism associated with European ancestry in northern Canada (Lehnert et al., 2019a).

481   The Ssa01/Ssa23 chromosomal translocation, previously associated with introgression

482   from European Atlantic Salmon into northern Canada (Lehnert et al. 2019a), was found to be

483   polymorphic within Placentia Bay and appeared to be a significant factor contributing to genetic

484   structuring in this region. Genetic variation of outlier loci within the outlier block regions

485   identified on chromosomes Ssa01 and Ssa23 showed three distinct clusters, a pattern observed by

486   Lehnert et al. (2019a) and consistent with a chromosomal rearrangement. Karyotype frequencies

487   showed a longitudinal clinal pattern. Populations on the Avalon Peninsula were predominately

488   composed of individuals with the standard European karyotype (homozygous non-translocated;

489   Ssa01p/q and Ssa23) whereas populations at the head of the bay and on the Burin Peninsula were

490   predominately composed of individuals with the standard North American karyotype

491   (homozygous translocated; Ssa01q and Ssa01p/Ssa23). Interestingly, Lehnert et al. (2019a) found

492   no individuals with the standard European karyotype south of Labrador, although sampling was

493   limited to only four populations in Newfoundland located west of the Burin Peninsula. While

494   long read nanopore sequencing is required to confirm the presence of a translocation in these

495   populations, this finding strongly supports a hypothesis of trans-Atlantic secondary contact in

496   Placentia Bay.

497   Observed patterns of genetic diversity indicated the standard North American karyotype

498   has reduced genetic diversity relative to the standard European karyotype. Furthermore, pairwise

499   comparisons of linkage disequilibrium between karyotypes suggested greater suppression of

500   recombination between the standard North American karyotype and heterokaryotype than

501   between the standard European karyotype and heterokaryotype. This finding is consistent with

502   reports of reduced frequency of recombination and a shift in the distribution of recombination

503   towards the distal ends of chromosomes in fused homokaryotypes and, to a lesser extent,

504   heterokaryotypes (Bidau et al., 2001; Castiglia & Capanna, 2002; Dumas & Britton-Davidian,

505   2002; Guerrero, & Kirkpatrick, 2014). While North American salmon generally have low levels

506   of European ancestry (~ 3% genome-wide), individuals with the standard European karyotype

507   have been reported to have high levels of European ancestry (> 50%) within the outlier block

508   regions on Ssa01 and Ssa23 (Lehnert et al., 2019a). Given that the SNP array was developed

509   using European Atlantic Salmon (Barson et al., 2015), it is possible inferences about diversity

510   may be influenced by ascertainment bias. However, the dataset used here was based on a subset

511   of polymorphic loci and using a similar array and methodology Bradbury et al. (2015) concluded

512   the observed pattern in genetic diversity along southern Newfoundland was the result of

513   historical processes with minimal influence of ascertainment bias.

514   Interestingly, the outlier block region identified on chromosome Ssa23 (0 – 9.5 Mbp) was

515   larger in size than that reported by Lehnert et al. (2019a) perhaps suggesting multiple secondary

516   contact events may have occurred during the colonization of North America following the last

517   glacial maximum, a hypothesis for which Rougemont & Bernatchez (2018) found some support.

518   Moreover, the larger outlier blocks found here may suggest a more recent secondary contact

519   event in Newfoundland compared to northern regions (Labrador). This highlights the need for

520   future studies on the demographic and evolutionary history of Atlantic Salmon in Canada. While

521   other studies have identified evidence that secondary contact influences differentiation range-

522   wide (Lehnert et al., 2019a), we found variation in the Ssa01/Ssa23 chromosomal translocation is

523   significantly associated with genome-wide population structure demonstrating the importance of

524   the Ssa01/Ssa23 chromosomal translocation to fine-scale structuring within Placentia Bay and

525   suggesting the translocation may influence gene flow through incompatibilities or adaptive

526   differences between karyotypes.

527

528   **4.2 Environment correlated with chromosomal translocation**

529   Geographic regions of post-glacial secondary contact can provide opportunities to

530   investigate the evolution and maintenance of chromosomal structural variation and its role in

531   adaptive divergence (Tigano & Friesen, 2016; Lee et al., 2017). Secondary contact events can

532   generate polymorphism in standing variation, which can then be selected upon in a heterogenous

533   environment (Alcala & Vuilleumier, 2014; Marques et al., 2019). Genomic architecture is an

534   underappreciated source of variation on which selection can act (Wellenreuther et al., 2019).

535   Chromosomal structural variants may be adaptive due to spatially and/or temporally varying

536   selection on: i) breakpoints or position effects which cause gene disruption or alter expression

537   (Corbett-Detig, 2016; Puerma, Orengo, & Aguadé, 2016), ii) recombination rate (McDonald,

538   Rice, & Desai, 2016), or iii) alleles captured or accumulated (Wright, 1931; Coyne & Orr, 2004;

539   Fuller et al., 2019). As such, chromosomal structural variants are expected to clearly delineate the

540   genetic boundaries between parapatric populations that straddle an ecotone (Slatkin, 1975;

541   Kirkpatrick & Barton, 2006). Using a fine-spatial scale approach we identified a cline in

542   translocation karyotype that aligned with an environmental gradient consistent with a hypothesis

543   of adaptive significance.

544   Placentia Bay, a long (125 km) and deep (240 m) embayment in southeastern

545   Newfoundland, spans 145 km at the mouth and narrows towards the head of the bay where

546   summer temperatures are warmer relative to the mouth of the bay (Fisheries and Oceans Canada,

547   2007). Genotype-environment analysis (redundancy analysis; RDA) indicated temperature range

548   and seasonality best explained the observed spatial genetic structure and highlighted a strong

549   association with the Ssa01/Ssa23 chromosomal translocation. Although the use of air temperature

550   as a proxy for freshwater temperature may not be accurate, particularly across small spatial scales

551   (Hansen, Read, Hansen, & Winslow, 2016), previous work in the region has reported a strong

552   correspondence between air and water temperatures (Bradbury et al., 2014). Furthermore, a

553   significant correlation between translocation frequency and temperature was found, indicating,

554   that like inversions, translocations have the potential to be adaptive, a finding supported by

555   evidence of signatures of positive selection acting on both the standard North American and

556   standard European karyotypes (Lehnert et al., 2019a). Taken together, these findings suggest the

557   standard North American karyotype is adaptive in North America, however, within secondary

558   contact zone(s) where introgression has occurred, the standard European karyotype also confers a

559   locally adaptive advantage, presumably by adding to standing variation on which selection acts

560   within a heterogenous landscape over a fine-spatial scale. Alternatively, temperature-aligned

561   population structure could be the result of demographic history. Chromosomal structural variants

562   may have been pre-adapted to differing temperature regimes and aligned themselves along the

563   currently observed cline in temperature during post-glacial colonization; consistent with a

564   hypothesis of niche coupling (Knowles, Carstens, & Keat, 2007). Regardless of the influence of

565   colonization history, a significant correlation between contemporary fine-scale population

566   structure and temperature was observed.

567   Local adaptation has been recognized as an important evolutionary process in salmonids

568   (reviewed in Taylor, 1991; Garcia de Leaniz et al., 2007) with temperature often identified as the

569   dominant factor structuring populations (Larson, Lisi, Seeb, Seeb, & Schindler, 2016).

570   Temperature has been shown to directly influence metabolic and growth rate (Burgerhout et al.,

571   2017; Stehfest et al., 2017; Vikeså, Nankervis, & Hevrøy, 2017), age at smoltification and

572   maturation (Mangel, 1994; Minns et al., 1995; Friedland, 1998), proportion of precocial parr in

573   Atlantic Salmon populations (Valiente et al., 2005; Yates et al. 2015), migration timing (Jonsson

574   & Jonsson, 2018), and fitness and survival through oxidative stress (Birnie-Gauvin, Costantini,

575   Cooke, & Willmore, 2017). While some evidence suggests a difference in proportion of precocial

576   males (Dalley, Andrew, & Green, 1983) between the mouth and head of Placentia Bay, little is

577   known about the life history and ecology of salmon at this spatial scale in this region.

578   While our results suggest an association between translocation frequency and

579   temperature, we acknowledge that other unmeasured variables that covary with temperature may

580   contribute to the genetic structure observed (Storfer et al., 2006). Inclusion of additional

581   environmental parameters, such as pH and/or geological characteristics (Bourret et al., 2013;

582   Bradbury et al., 2014), and pathogen or parasite diversity (Dionne, Miller, Dodson, &

583   Bernatchez, 2009), may provide further insight into the mechanisms influencing spatial structure

584   in the region. Although, notably, in regions such as Labrador, previous work has found a higher

585   frequency of the standard European karyotype within populations within a large marine

586   embayment (Lake Meville) where temperatures are warmer compared to coastal populations with

587   a lower frequency of the standard European karyotype (Sylvester et al., 2018; Lehnert et al.,

588   2019a). While this association has not been formally tested, it highlights another region in North

589   America where polymorphism of the Ssa01/Ssa23 chromosomal translocation may align with

590   clinal variation in temperature. Although these relationships appear to operate in different

591   directions, this may further support the role of multiple secondary contact events in parts of

592   Canada from different regions of Europe.

593

4.3 Chromosomal translocation exhibits temporal stability across ecotone

Translocation frequency was found to be temporally stable across the two discrete years sampled. A pronounced transition in translocation frequency was observed between Ship Harbour (SHI) and Fair Haven Brook (FHB) on the Avalon Peninsula, however, this transition was less apparent on the Burin Peninsula, where Northwest Mortier (NMB) and Big Salmonier (BSA), rivers located in an intermediary zone of clinal variation, were found to significantly differ in translocation frequency between 2017 and 2018. While maintenance of polymorphism and temporal stability suggest the Ssa01/Ssa23 chromosomal translocation is adaptive, it is plausible that the Ssa01/Ssa23 chromosomal translocation is neutral or near-neutral and polymorphism persists due to demographic factors such as low gene flow and low effective population size in region (Palstra et al., 2007; Bradbury et al., 2015) and drift. Alternatively, polymorphism of the Ssa01/Ssa23 chromosomal translocation may be maintained, not because the variants represent adaptations to divergent habitats, but because the homozygous translocated karyotype carries harmful recessive mutations as suggested by Jay et al. (2019) in *Heliconious numata*. Future work should examine transposable element (TE) dynamics and the rate of non-synonymous to synonymous substitution (dN/dS) within the translocated region.

610

4.4 Functional significance and gene annotations

We identified biological processes which were over-represented using genes within the outlier block regions on Ssa01 and Ssa23 that were located near environmentally associated SNPs. KEGG pathway analysis found enrichment of the insulin signalling pathway in both 2017 and 2018. In addition, analysis of gene ontology found over-representation of biological

616 processes primarily related to regulation of metabolic processes, and immune response. The

617 insulin signalling pathway may relate to both metabolic processes (Babbitt, Warner, Fedrigo,

618 Wall, & Wray, 2010; Zhang et al. 2018) and immunity (Yada & Tort, 2016; Cheng et al., 2017;

619 Wang et al., 2019).

620   In salmon, genes and/or biological processes related to metabolic processes and immunity

621 can be influenced by environmental factors, such as temperature (Dionne, Miller, Dodson, Caron,

622 & Bernatchez, 2007; Beauregard et al., 2013). Metabolic differences in salmon populations under

623 different temperature regimes have been reported; salmon in warmer conditions grow faster and

624 migrate to sea at a younger age (Power, 1981; Metcalfe & Thorpe, 1990) while salmon in cooler

625 environments exhibit higher growth rate and more efficient metabolic processes (Nicieza et al.,

626 1994). In Atlantic Salmon, precocial male parr are common in Newfoundland (Dalley et al.

627 1983), and their occurrence can be influenced by temperature (Valiente et al., 2005; Yates et al.

628 2015).

629   Temperature regime has also been correlated with bacterial diversity and as such genetic

630 diversity for immune-related genes (Dionne et al., 2007, 2008) and is thought to be involved in

631 local adaptation to different pathogen communities (Bourret et al., 2013). Parasites have played a

632 major role in mortality of wild fish in Newfoundland (Khan, 2009) with outbreaks and mortality

633 of proliferative kidney disease (PKD) being seasonal and temperature dependent in salmonids

634 (Sterud et al., 2007). Overall, these processes point to potential adaptive associations with

635 temperature but remain speculative, and experimental work is needed to better understand these

636 relationships.

637

638 **4.5 Conservation and management implications**

639   Atlantic Salmon in southern Newfoundland have undergone significant declines in

640   abundance over the last few decades (Chaput et al., 2012; Lehnert et al., 2019b) and are currently

641   managed as a single designatable or evolutionarily significant unit (COSEWIC, 2010). Our

642   results clearly demonstrate two genetic clusters and provide strong evidence that an adaptive

643   chromosomal translocation associated with trans-Atlantic secondary contact drives fine-scale

644   population structure in the region. Placentia Bay is of particular interest in that it is a geographic

645   region of post-glacial secondary contact and as such provides an opportunity to investigate the

646   evolution and maintenance of chromosomal structural variation and its role in adaptive

647   divergence because evolutionary dynamics of chromosomal structural variants differ from other

648   parts of the genome, (Tigano & Friesen, 2016; Lee et al., 2017; Wellenreuther & Bernatchez,

649   2018; Mérot, Oomen, Tigano, & Wellenreuther, 2020). While polymorphism in chromosomal

650   structural variation, such as the Ssa01/Ssa23 chromosomal translocation characterized here, may

651   complicate the process of delineating evolutionarily significant units, particularly when the

652   relative fitness consequences are unclear, it can be important to consider genomic architecture

653   underlying adaptive phenotype or life history variation when predicting the consequences of

654   environmental disturbance and climatic change (Oomen, Kuparinen, & Hutchings, 2020).

655

656

657   **5 CONCLUSIONS**

658   Species and populations adapt through selection imposed by spatially and temporally

659   heterogenous environments on new mutation or standing genetic variation (Wright, 1931; Coyne

660   & Orr, 2004). Gene flow is an important source of standing genetic variation (Tigano & Friesen,

661   2016) promoting adaptation through the re-introduction of previously lost variation (Rieseberg,

662   2009) and the introgression of novel genetic variants and allelic combinations among meta-

663   populations (Poelstra, Richards, & Martin, 2018). The Ssa01/Ssa23 chromosomal translocation

664   (Brenna-Hansen et al., 2012) has recently been found to be polymorphic within secondary contact

665   zones in North America (Lehnert et al., 2019a). This study further supports secondary contact

666   with European introgression into Atlantic Salmon populations along southeastern Newfoundland

667   and highlights the importance of secondary contact in shaping population genetic structure.

668   Effects of chromosomal structural variants are expected to be most pronounced when fixed in

669   populations prior to secondary contact, with subsequent reproductive isolation maintained by

670   adaptive change involving many genes with small fitness effects (Feder, Nosil, & Flaxman,

671   2014). Here, we found evidence of an adaptive chromosomal rearrangement and a cline in

672   translocation frequency aligned with a cline in temperature. These findings suggest the standard

673   North American karyotype is broadly adaptive in North America, however, within secondary

674   contact zone(s) where introgression of the standard European karyotype has occurred, the

675   standard European karyotype also confers an adaptive advantage in local populations. Future

676   work should explore the roles of demography and drift, monitor clinal stability of translocation

677   frequency over an extended period of time to investigate the evolution and maintenance of

678   putatively adaptive translocation in the wild, and use direct temperature measurements and

679   common-garden experiments to investigate differential gene expression between

680   homokaryotypes. This study highlights the importance of chromosomal structural variation as a

681   source of standing variation on which selection can act.

682

683

684

692

693

694

695

696

697

698

699

700

701

702

703

704

705

706

707

REFERENCES

Alcala, N., & Vuilleumier, S. (2014). Turnover and accumulation of genetic diversity across large time-scale cycles of isolation and connection of populations. *Proceedings of the Royal Society B*, **281**(1704), https://doi.org/10.1098/rspb.2014.1369.

Alexa, A., Rahnenführer, J., & Lengauer, T. (2006). Improved scoring of functional groups from gene expression data by decorrelating GO graph structure. *Bioinformatics*, **22**(13), 1600– 1607.

Alexander, D. H., Novmbre, J., & Lange, K. (2009). Fast model-based estimation of ancestry in unrelated individuals. *Genome Research*, **19**, 1655 – 1664.

Babbitt, C. C., Warner, L. R., Fedrigo, O., Wall, C. E., & Wray, G. A. (2010). Genomic signatures of diet-related shifts during human origins. *Proceedings of the Royal Society B*, **278**(1708), https://doi.org/10.1098.rspb/2010.2433.

Balanyà, J., Huey, R. B., Gilchrist, G. W., & Serra, L. (2009). The chromosomal polymorphism of *Drosophila subobscura*: a microevolutionary weapon to monitor global change. *Heredity*. **103**, 364 – 367.

Barson, N. J., Aykanat, T., Hindar, K., Baranski, M., Bolstad, G. H., Fiske, P., … & Primmer, C. R. (2015). Sex-dependent dominance at a single locus maintains variation in age at maturity in salmon. *Nature*, **528**, 405– 408.

Beauregard, D., Enders, E., & Boisclair, D. (2013). Consequences of circadian fluctuations in water temperature on the standard metabolic rate of Atlantic salmon parr (*Salmo salar*). *Canadian Journal of Fisheries and Aquatic Sciences*, **70**(7), 1072 – 1081.

Bidau, C. J., Giménez, M. D., Palmer, C. L., & Searle, J. B. (2001). The effects of Robertsonian fusion on chiasma frequency and distribution in the house mouse (*Mus musculus domesticus*) from a hybrid zone in northern Scotland. *Heredity*, **87**, 305 – 313.

Bidau, C. J., & Martí, D. A. (2002). Geographic distribution of Robertsonian fusions in *Dichroplus pratensis*, (Melanoplinae, Acrididae): the central-marginal hypothesis reanalysed. *Cytogenetic and Genome Research*, **96**, 66 – 74.

Bidau, C. J., Miño, C. I., Castillo, E. R., & Martí, D. A. (2012). Effects of abiotic factors on the geographic distribution of body size variation and chromosomal polymorphisms in two neotropical grasshopper species (*Dichroplus*: Melanoplinae: Acrididae). *Psyche*, https://doi.org/10.1155/2012/863947.

Birnie-Gauvin, K., Costantini, D., Cooke, S. J., & Willmore, W. G. (2017). A comparative and evolutionary approach to oxidative stress in fish : a review. *Fish and Fisheries*, **18**(5), 928 – 942. https://doi.org/10.1111/faf.12215.

752 Bourret, V., Dionne, M., Kent, M. P., Lien, S., & Bernatchez, L. (2013). Landscape genomics in
753 Atlantic salmon (*Salmo salar*) searching for gene-environment interactions driving local
754 adaptation. *Evolution*, **67**(12), 3469 – 3487.

756 Bradbury, I. R., Hamilton, L. C., Robertson, M. J., Bourgeois, E., Mansour, A., & Dempson, B.,
757 (2014). Landscape structure and climatic variation determine Atlantic salmon genetic
758 connectivity in the Northwest Atlantic. *Canadian Journal of Fisheries and Aquatic Sciences*,
759 **71**(2), 246 – 258.

761 Bradbury, I. R., Hamilton, L. C., Dempson, B., Robertson, M. J., Bourret, V., Bernatchez, L., &
762 Verspoor, E. (2015). Transatlantic secondary contact in Atlantic salmon, comparing
763 microsatellites, a single nucleotide polymorphism array and restriction-site associated DNA
764 sequencing for the resolution of complex spatial structure. *Molecular Ecology*, **24**(20), 5130 –
765 5144.

767 Brenna-Hansen, S., Li, J., Kent, M. P., Boulding, E. G., Dominik, S., Davidson, W. S. & Lien, S.
768 (2012). Chromosomal differences between European and North American Atlantic salmon
769 discovered by linkage mapping and supported by fluorescence *in situ* hybridization analysis.
770 *BMC Genomics*, **13**, 432.

772 Burgerhout, E. (2017). Genetic background and embryonic temperature affect DNA methylation
773 and expression of *myogenin* and muscle development in Atlantic salmon (Salmo salar). *PLoS*
774 *One*, **12**(6): e0179918.

776 Campbell, C. R., Poelstra, J. W., & Yoder, A. D. (2018). What is speciation genomics? The roles
777 of ecology, gene flow, and genomic architecture in the formation of species. *Biological Journal*
778 *of the Linnean Society*, **124**(4), 1 – 23.

780 Castiglia, R., & Capanna, E. (2002). Chiasma repatterning across a chromosomal hybrid zone
781 between chromosomal races of *Mus musculus domesticus*. *Genetica*, **114**, 35 – 40.

783 Cayuela, H., Dorant, Y., Merot, C., Laporte, M., Normandeau, E., Gagnon-Harvey, S., Sirois, P.,
784 & Bernatchez, L. (2020). Thermal adaptation rather than demographic history drives genetic
785 structure inferred by copy number variants in a marine fish. *BioRkiv,*
786 https://doi.org/10.1101/2020.04.05.026443.

788 Chang, C. C., Carson, C. C., Tellier, L. C. A. M., Vattikuti, S., Purcell, S. M., & Lee, J. J. (2015).
789 Second-generation PLINK: rising to the challenge of larger and richer datasets. *GigaScience*,
790 **4**(7), doi:10.1186/s13742-015-0047-8.

792 Chaput, G. (2012). Overview of the status of Atlantic salmon (*Salmo salar*) in the North Atlantic
793 and trends in marine mortality. *ICES Journal of Marine Science*, **69**, 1538 – 1548.

795 Charlesworth, B. (1985). Recombination, genome size and chromosome number. In T. Cavalier-
796 Smith (Ed.), *The evolution of genome size* (pp 489 – 513). John Wiley & Sons, Chichester.

797

798 Cheng, C-H., Ye, C-X., Guo, Z-X., & Wang, A-L. (2017). Immune and physiological responses
799 of pufferfish (*Takifugu obscurus*) under cold stress. *Fish & Shellfish Immunology*, **64**, 137 – 145.

800

801 Corbett-Detig, R. B. (2016). Selection on inversion breakpoints favors proximity to pairing
802 sensitive sites in *Drosophila melanogaster*, *Genetics*, **204**(1), 259 – 265.

803

804 COSEWIC. (2010). *COSEWIC assessment and status report on the Atlantic Salmon Salmo salar*
805 *(Nunavik population, Labrador population, Northeast Newfoundland population, South*
806 *Newfoundland population, Southwest Newfoundland population, Northwest Newfoundland*
807 *population, Quebec Eastern North Shore population, Quebec Western North Shore population,*
808 *Anticosti Island population, Inner St. Lawrence population, Lake Ontario population, Gaspé-*
809 *Southern Gulf of St. Lawrence population, Eastern Cape Breton population, Nova Scotia*
810 *Southern Upland population, Inner Bay of Fundy population, Outer Bay of Fundy population) in*
811 *Canada*. Committee on the Status of Endangered Wildlife in Canada. Ottawa. xlvii + 136 pp.

812

813 Coyne, J. A., & Orr, H. A. (2004). *Speciation*. Sinauer, Sunderland, MA.

814

815 Dalley, E. L., Andrews, C. W., & Green, J. M. (1983). Precocious male Atlantic salmon parr
816 (*Salmo salar*) in insular Newfoundland. *Canadian Journal of Fisheries and Aquatic Science*,
817 **40**(5), 647 – 652.

818

819 Dionne, M., Miller, K. M., Dodson, J. J., Caron, F., & Bernatchez, L. (2007). Clinal variation in
820 MHC diversity with temperature: evidence for the role of host-pathogen interaction on local
821 adaptation in Atlantic salmon. *Evolution*, **61**(9), 2154 – 2164.

822

823 Dionne, M., Caron, F., Dodson, J. J., & Bernatchez, L. (2008). Landscape genetics and
824 hierarchical genetic structure in Atlantic salmon: the interaction of gene flow and local
825 adaptation. *Molecular Ecology*, **17**(10), 2382 – 2396.

826

827 Dionne, M., Miller, K. M., Dodson, J. J., & Bernatchez, L. (2009). MHC standing genetic
828 variation and pathogen resistance in wild Atlantic salmon. *Philosophical Transactions of the*
829 *Royal Society B*, **364**(1523), https://doi.org/10.1098/rstb.2009.0011.

830

831 Dobigny, G., Britton-Davidian, J., & Robinson, T. J. (2017). Chromosomal polymorphism in
832 mammals: an evolutionary perspective. *Biological Reviews*, **92**(1), 1 – 21.

833

834 Dobzhansky, T. (1951). Genetics and the origin of species (3rd ed.) Columbia University Press.

835

836 Dumas, D., & Britton-Davidian, J. (2002). Chromosomal rearrangements and evolution of
837 recombination: comparison of chiasma distribution patterns in standard and Robertsonian
838 populations of the house mouse. *Genetics*, **162**(3), 1355 – 1366.

839

840 Feder, J. L., Nosil, P., & Flaxman, S. M. (2014). Assessing when chromosomal rearrangements
841 affect the dynamics of speciation: implications from computer simulations. *Frontiers in Genetics*,
842 https://doi.org/10.3389/fgene.2014.00295.

844 Felsentein, J. (1976). The theoretical population genetics of variable selection and migration.
845 *Annual Review of Genetics*, **10,** 253 – 280.

847 Fick, S. E., & Hijmans, R. J. (2017). WorldClim 2: New 1-km spatial resolution climate surfaces
848 for global land areas. *International Journal of Climatology*, **37**(12), 4302– 4315.

850 Fisheries and Ocean Canada (2007). *Placentia Bay integrated management plan*. Fisheries and
851 Oceans Canada. Retrieved from the Fisheries and Marine Institute of Memorial University of
852 Newfoundland website:
853 https://www.mi.mun.ca/media/marineinstitutewwwmimunca/mi/programsandcourses/marinespati
854 alplanning/files/PBIMCIntegratedManagementPlan.pdf

856 Friedland, K. D. (1998). Ocean climate influences on critical Atlantic salmon (Salmo salar) life
857 history events. *Canadian Journal of Fisheries and Aquatic Science*, **55**(Supplement 1), 119 –
858 130.

860 Fuller, Z. L., Koury, S. A., Phadnis, N., & Schaeffer, S. W. (2019). How chromosomal
861 rearrangements shape adaptation and speciation: case studies in *Drosophila pseudoobscura* and
862 its sibling species *Drosophila persimilis*. *Molecular Ecology*, **28**(6), 1238 – 1301.

864 Garcia de Leaniz, C., Fleming, I. A., Einum, S., Verspoor, E., Jordan, W. C., Consuegra, S., & …
865 Quinn, T. P. (2007). A critical review of adaptive genetic variation in Atlantic salmon:
866 implications for conservation. *Biological Reviews*, **82**(2), 173 – 211.

868 Goudet, J. (2005). HIERFSTAT, a package for R to compute and test hierarchical *F*-statistics.
869 *Molecular Ecology Notes*, **5**(1), 184 – 186.

871 Guerrero, R. F., & Kirkpatrick, M. (2014). Local adaptation and the evolution of chromosomes
872 fusions. *Evolution*, **68**(10), 2747 – 2756.

874 Hansen, G. J. A.*,* Read, J. S.*,* Hansen, J. F.*, &* Winslow, L. A. (2016). Projected shifts in fish
875 species dominance in Wisconsin lakes under climate change. *Global Change Biology,* **23**(4)*,*
876 1463 – 1476.

878 Hartley, S. (1988). Cytogenetic studies of Atlantic salmon, *Salmo salar* L., in Scotland. *Journal*
879 *of Fish Biology*, **33**, 735– 740.

881 Hewitt, G. (2000). The genetic legacy of the Quaternary ice ages. *Nature,* **405***,* 907 – 913*.*

883   Huang, K., Andrew, R. L., Owens, G. L., Ostevik, K., L., Rieseberg, L. H., (2019**)**. Multiple
884   chromosomal inversions contribute to adaptive divergence of a dune sunflower ecotype. *BioRkiv*,
885   https://doi.org/10.1101/829622.

886

887   Jay, P., Whibley, A., Frézal, L., Rodríguez de Cara M. A., Nowell, R. W., Mallet, J., … & Joron,
888   M. (2018). Supergene evolution triggered by the introgression of a chromosomal inversion.
889   *Current Biology*, https://doi.org/10.1016/j.cub.2018.04.072.

890

891   Jay, P., Chouteau, M., Whibley, A., Bastide, H., Llaurens, V., Parrinello, H., & Joron, M. (2019).
892   Mutation accumulation in chromosomal inversions maintains wing pattern polymorphism in a
893   butterfly. *BioRxiv*, https://doi.org/10.1101/736504.

894

895   Jonsson, B., & Jonsson, N. (2018). Egg incubation temperature affects the timing of the Atlantic
896   salmon *Salmo salar* homing migration. *Journal of Fish Biology*, **93**(5), 1016 – 1020.

897

898   Kanehisa, M., Goto, S., Sato, Y., Furumichi, M., & Tanabe, M. (2012). KEGG for integration
899   and interpretation of large-scale molecular data sets. *Nucleic Acids Research*, **40**(1), 109– 114.

900

901   Kapun, M., Fabian, D. K., Goudet, J., & Flatt, T. (2016). Genomic evidence for adaptive
902   inversion clines in *Drosophila melanogaster*. *Molecular Biology and Evolution*, **33**(5), 1317 –
903   1336.

904

905   Kennington, W. J., & Hoffmann, A. A. (2013). Patterns of genetic variation across inversions:
906   geographic variation in the *In*(*2L*)*t* inversion in populations of *Drosophilia melanogaster* from
907   eastern Australia. *BMC Evolutionary Biology*, **13**, 100.

908

909   Khan, R. A. (2009). Parasites causing disease in wild and cultured fish in Newfoundland.
910   *Icelandic Agricultural Sciences*, **22**, 29 – 35.

911

912   King, M. (1993). *Species evolution: the role of chromosomal change*. Cambridge University
913   Press, Cambridge, U. K.

914

915   King, T. L., Verspoor, E., Spidle, A. P., Gross, R., Phillips, R. B., Koljonen, M. L., & …
916   Morrison, C. L. (2007). Biodiversity and population structure. In E. Verspoor, L. Stradmeyer, &
917   J. Nielsen (Eds.), *The Atlantic Salmon: Genetics, conservation and management* (pp. 117– 166).
918   Oxford, UK: Blackwell Publishing Ltd.

919

920   Kirkpatrick, M., & Barton, N. (2006). Chromosome inversions, local adaptation and speciation.
921   *Genetics*, **173**, 419 – 434.

922

923   Knowles, L. L.*,* Carstens, B. C.*, &* Keat, M. L. (2007). Coupling genetic and ecological-niche
924   models to examine how past population distributions contribute to divergence*. Current Biology,*
925   **17**(11)*,* 940–946*.*

926

927 Lamichhaney, S., Fan, G., Widemo, F., Gunnarsson, U., Schwochow Thalmann, D., Hoeppner,
928 M. P., & … Andersson, L. (2016). Structural genomic changes underlie alternative reproductive
929 strategies in the ruff (*Philomachus pugnax*). *Nature Genetics*, **48**, 84 – 88.
930
931 Larson, W. A*., Lisi, P. J*., Seeb, J. E*., Seeb, L. W*., &* Schindler, D. E. (2016). Major
932 histocompatibility complex diversity is positively associated with stream water temperatures in
933 proximate populations of sockeye salmon. *Journal of Evolutionary Biology,* **29**(9)*, 1846 – 1859.*
934
935 Lee, C-R., Wang, B., Mojica, J. P., Mandáková, T., Prasad, K. V. S. K., Goicoechea, J. L., … &
936 Mitchell-Olds, T. (2017). Young inversion with multiple linked QTLs under selection in a hybrid
937 zone. *Nature Ecology and Evolution*, **1**:0119. doi:10.1038/s41559-017-0019
938
939 Lehner, B., Verdin, K., & Jarvis, A. (2008). New global hydrography derived from spaceborne
940 elevation data. *EOS*, **89**(10), 93 – 94.
941
942 Lehnert, S. J., Bentzen, P., Kess, T., Lien, S., Horne, J. B., Clement, M., & Bradbury, I. R.
943 (2019a). Chromosome polymorphisms track trans-Atlantic divergence and secondary contact in
944 Atlantic salmon. *Molecular Ecology*, **28**(8), 2074 – 2087.
945
946 Lehnert, S. J., Kess, T., Bentzen, P., Kent, M. P., Lien, S., Gilbey, J., …. Bradbury, I. R. (2019b).
947 Genomic signatures and correlates of widespread population declines in salmon. *Nature*
948 *Communications*. https://doi.org/10.1038/s41467-019-10972-w
949
950 Luu, K., Bazin, E., & Blum, M. G. (2017). pcadapt: An R package to perform genome scans for
951 selection based on principal component analysis. *Molecular Ecology Resources*, **17**, 67– 77.
952
953 McAllister, B. F. (2003). Sequence differentiation associated with an inversion on the neo-X
954 chromosome of *Drosophila americana*. *Genetics*, **165**(3), 1317 – 1328.
955
956 McCartney-Melstad, E., Vu, J.K., & Shaffer, H.B. (2018). Genomic data recover previously
957 undetectable fragmentation effects in an endangered amphibian. *Molecular Ecology*, **27**(22),
958 4430 – 4443.
959
960 McDonald, M. J*., Rice, D. P*., &* Desai, M. M. (2016). Sex speeds adaptation by altering the
961 dynamics of molecular evolution*. Nature,* **531**(7593), 233–236.
962
963 Mangel, M. (1994). Climate change and salmonid life history variation. *Deep-Sea Research*, **41**,
964 75 – 106.
965
966 Marques, D. A., Meier, J. I., & Seehausen, O. (2019). A combinatorial view on speciation and
967 adaptive radiation. *Trends in Ecology and Evolution*, **34**(6), 531 – 544.
968
969
970

Mérot, C., Berdan, E. L., Babin, C., Normandeau, E., Wellenreuther, M., & Bernatchez, L. (2018). Intercontinental karyotype-environment parallelism supports a role for a chromosomal inversion in local adaptation in a seaweed fly. *Proceedings of the Royal Society B*, **285**(1881), https://doi.org/10.1098/rspb.2018.0519

Mérot, C., Oomen, R. A., Tigano, A., & Wellenreuther, M. (2020). A roadmap for understanding the evolutionary significance of structural genomic variation. *Trends in Ecology & Evolution*, (in press). https://doi.org/10.1016/j.tree.2020.03.002.

Metcalfe, N. B., & Thorpe, J. E. (1990). Determinants of geographical variation in the age of seaward-migrating salmon, *Salmo salar*. *Journal of Animal Ecology*, **59**(1), 135 – 145.

Minns, C. K., Randall, R. G., Chadwick, E. M. P., Moore, J. E., & Green, R. (1995). In Climate change and northern fish populations. Edited by R. J. Beamish, *Canadian Special Publication of Fisheries and Aquatic Sciences*, **121**, 699 – 708.

Nei, M. (1972). Genetic distance between populations. *The American Naturalist*, **106**, 283 – 292.

Nei, M. (1987). *Molecular evolutionary genetics*. Columbia University Press, New York.

Nicieza, A G., Reyes-Gavilán, F. G., & Braña, F. (1994). Differentiation in juvenile growth and bimodality patterns between northern and southern populations of Atlantic salmon (*Salmo salar* L.). *Canadian Journal of Fisheries and Aquatic Sciences*, **72**(9), 1603 – 1610.

Nilsson, J., Gross, R., Asplund, T., Dove, O., Jansson, H., Kellonieni, J. & … . Lumme, J. (2001). Matrilineal phylogeography of Atlantic salmon (*Salmo salar* L.) in Europe and postglacial colonization of the Baltic Sea area. *Molecular Ecology,* **10**(1): 89 – 92.

Oksanen, J., Guillaume Blanchet, F., Friendly, M., Kindt, R., Legendre, P., McGlinn, D., … & Wagner, H. (2017). vegan: Community ecology package. *R package version 2.4-5*. Retrieved from https://github.com/vegandevs/vegan

Oomen, R. A., Kuparinen, A., & Hutchings, J. A. (2020). Consequences of single-locus and tightly linked genomic architectures for evolutionary responses to environmental change. *BioRxiv*, https://doi.org/10.1101/2020.01.31.928770.

Palstra, F. P., O'Connell, M. F., & Ruzzante, D. E. (2007). Population structure and gene flow reversals in Atlantic salmon (*Salmo salar*) over contemporary and long-term temporal scales: effects of population size and life history. *Molecular Ecology*, **16**(21), 4504 – 4522.

Pante, E., & Simon-Bouhet, B. (2013). marmap: a package for importing, plotting and analyzing bathymetric and topographic data in R. *PLoS One*, **8**(9): e73051.

1014   Pembleton, L. W., Cogan, N. O. I., & Forster, J. W. (2013). StAMPP: an R package for
1015   calculation of genetic differentiation and structure of mixed-ploidy level populations. *Molecular*
1016   *Ecology Resources*, **13**(5), 946 – 952.

1017
1018   Phillips, R., & Ráb, P. (2001). Chromosome evolution in the Salmonidae (Pisces): an update.
1019   *Biological Reviews*. **76**, 1 – 25.

1020
1021   Poelstra, J. W., Richards, E. J., & Martin, C. H. (2018). Speciation in sympatry with ongoing
1022   secondary gene flow and a potential olfactory trigger in a radiation of Cameroon cichlids.
1023   *Molecular Ecology*, **27**(21), 4270 – 4288.

1024
1025   Porter, T. R., Riche, L. G., & Traverse, G. R. (1974). *Catalogue of rivers in insular*
1026   *Newfoundland, vol. A.*, Department of the environment, St. John's, NL.

1027
1028   Power, G. (1981). Stock characteristics and catches of Atlantic salmon (Salmo salar) in Quebec,
1029   and Newfoundland and Labrador in relation to environmental variables. *Canadian Journal of*
1030   *Fisheries and Aquatic Sciences*, **38**(12), 1601 – 1611.

1031
1032   Puerma, E., Orengo, D. J., & Aguadé, M. (2016). Multiple and diverse structural changes affect
1033   the breakpoint regions of polymorphic inversions across the *Drosophila* genus. *Scientific*
1034   *Reports*, **6**, 36248. https://doi.org/10.1038/srep36248

1035
1036   Purcell, S., Neale, B., Todd-Brown, K., Thomas, L., Ferreira, M. A. R., Bender, D., … & Sham,
1037   P. C. (2007). PLINK: A tool set for whole-genome association and population-based linkage
1038   analyses. *The American Journal of Human Genetics*, **81**, 559– 575.

1039
1040   R Core Team. (2019). R: a language and environment for statistical computing. *R Foundation for*
1041   *Statistical Computing*, Vienna, Austria. http://www.R-project.org/

1042
1043   Quinlan, A. R.*, & Hall, I. M. (2010). BEDTools: A flexible suite of utilities for comparing
1044   genomic features. *Bioinformatics,* **26**(6)*, 841–842

1045
1046   Rajagopal, V. M. (2020). *ggman*: R package for Manhattan plots, GitHub repository
1047   https://github.com/drveera/ggman/

1048
1049   Rambaut, A. (2012). FigTree (Version 1.4). Retrieved from
1050   http://tree.bio.ed.ac.uk/software/figtree/

1051
1052   Rieseberg, L. H. (2001). Chromosomal rearrangements and speciation. *Trends in Ecology and*
1053   *Evolution*, **16**(7), 351 – 358.

1054
1055   Rieseberg, L. H. (2009). Evolution: replacing genes and traits through hybridization. *Current*
1056   *Biology*, **19**(3), R119-R122.
1057

Rougemont, Q., & Bernatchez, L. (2018). The demographic history of Atlantic salmon (*Salmo salar)* across its distribution range reconstructed from approximate Bayesian computations. *Evolution*, **72**(6), 1261 – 1277.

Samy, J. K. A., Mulugeta, T. D., Nome, T., Sandve, S. R., Grammes, F., Kent, M. P., … & Våge, D. I. (2020). SalmoBase: an integrated molecular data resource for Salmonid species. *BMC Genomics*, **18**, 482. Doi:10.1186/s12864-017-3877-1.

Savolainen, O., Lascoux, M., & Merilä, J. (2013). Ecological genomics of local adaptation. *Nature Reviews Genetics*, **14**, 807 – 820.

Schulter, D. (2009). Evidence for ecological speciation and its alternative. *Science*, **323**(5915), 737 – 741.

Sinclair-Waters, M., Bradbury, I. R., Morris, C. J., Lien, S., Kent, M. P. & Bentzen, P. (2018). Ancient chromosomal rearrangement associated with local adaptation of a postglacially colonized population of Atlantic cod in the northwest Atlantic. *Molecular Ecology*, **27**(2), 339 – 351.

Slatkin, M. (1975). Gene flow and selection in a two-locus system. *Genetics*, **81**(4), 787 – 802.

Stehfest, K. M., Carter, C. G., McAllister, J. D., Ross, J. D., & Semmens, J. M. (2017). Response of Atlantic salmon *Salmo salar* to temperature and dissolved oxygen extremes established using animal-borne environmental sensors. *Scientific Reports*, **7**, 4545, https://doi.org/10.1038/s41598-017-04806-2

Sterud, E., Forseth, T., Ugedal, O., Poppe, T. T., Jorgensen, A., Bruheim, T., … & Mo, T. A. (2007). Severe mortality in wild Atlantic salmon *Salmo salar* due to proliferative kidney disease (PKD) caused by *Tetracapsuloides bryosalmonae* (Myxozoa). Diseases of Aquatic Organisms, **77**, 191 – 198.

Storey, J. D., Bass, A. J., Dabney, A., & Robinson, D. (2015). qvalue: Q-value estimation for false discovery rate control. (R package 2.10.0). Vienna, Austria: R Foundation for Statistical Computing. Retrieved from http://github.com/jdstorey/qvalue

Storfer, A.*,* Murphy, M. A.*,* Evans, J. S.*,* Goldberg, C. S.*,* Robinson, S.*,* Spear, S. F.*, &...* Waits, L. P. (2006). Putting the 'landscape' in landscape genetics. *Heredity,* **98**(3)*,* 128 – 142.

Sturtevant, A. H. (1917). Genetic factors affecting the strength of linkage in *Drosophilia*. *Proceedings of the National Academy of Science USA*, **3**:555.

Sturtevant, A. H. (1938). The interrelations of inversions, heterosis and recombination. *The American Naturalist*, 72:742, 447 - 452.

1101　Sylvester, E.V.A., Beiko, R. G., Bentzen, P., Paterson, I., Horne, J. B., Watson, B., … &
1102　Bradbury, I.R. (2018). Environmental extremes drive population structure at the northern range
1103　limit of Atlantic salmon in North America. *Molecular Ecology*, **27**(20), 4026 – 4040.
1104
1105　Sylvester, E.V.A., Wringe, B.F., Duffy, S.J., Hamilton, L.C., Fleming, I.A., Castellani, M., … &
1106　Bradbury, I.R. (2019). Estimating the relative fitness of escaped farmed salmon offspring in the
1107　wild and modelling the consequences of invasion for wild populations. *Evolutionary*
1108　*Applications*, **12**(4), 705 – 717.
1109
1110　Taylor, E. B. (1991). A review of local adaptation in Salmonidae, with particular references to
1111　Pacific and Atlantic salmon. *Aquaculture*, **98**(1 – 3), 185 – 207.
1112
1113　Tigano, A., & Friesen, V. L. (2016). Genomics of local adaptation with gene flow. *Molecular*
1114　*Ecology*, **25**(10), 2144 – 2164.
1115
1116　Turner, S. D. (2014). Qqman: An R package for visualizing GWAS results using QQ and
1117　manhattan plots. *BioRxiv*, 005165.
1118
1119　Valiente, A. G., Juanes, F., & Garcia-Vazquez, E. (2005). Reproductive strategies explain genetic
1120　diversity in Atlantic salmon, *Salmo salar*. *Environmental Biology of Fishes*, **74**, 323 – 334.
1121
1122　Verspoor, E., McGinnity, P., Bradbury, I., & Glebe, B. (2015). The potential direct and indirect
1123　genetic consequences for native Newfoundland Atlantic salmon from interbreeding with
1124　European-origin farm escapes. *DFO Can. Sci. Advis. Sec. Res. Doc*. 2015/030. vii + 36 p.
1125
1126　Vikeså, V., Nankervis, L., & Hevrøy, E. M. (2017). Appetite, metabolism and growth regulation
1127　in Atlantic salmon (*Salmo salar* L.) exposed to hypoxia at elevated seawater temperature.
1128　*Aquaculture Research*, **48**(8), 4086 – 4101.
1129
1130　Wang, Y., Li, C., Pan, C., Liu, E., Zhao, X., & Ling, Q. (2019). Alterations to transcriptomic
1131　profile, histopathology, and oxidative stress in liver of pikeperch (*Sander lucioperca*) under heat
1132　stress. *Fish & Shellfish Immunology*, **95**, 659 – 669.
1133
1134　Warnes, G. R., Bolker, B., Bonebakker, L., Gentleman, R., Liaw, W. H. A., Lumley, T., ...
1135　Venables, B. (2016). gplots: Various R programming tools for plotting data (R package 3.0.1).
1136　Vienna, Austria: *R Foundation for Statistical Computing*.
1137
1138　Weir, B. S., & Cockerham, C. C. (1984). Estimating *F*-statistics for the analysis of population
1139　structure. *Evolution,* **38**(6), 1358 – 1370.
1140
1141　Wellband, K., Mérot, C., Linnansaari, T., Elliott, J. A, K., Curry, A., Bernatchez, L. (2019).
1142　Chromosomal fusion and life history-associated genomic variation contribute to within-river
1143　local adaptation of Atlantic salmon. *Molecular Ecology*, **28**(6), 1439 – 1459.
1144

1145 Wellenreuther, M., & Bernatchez, L. (2018). Eco-evolutionary genomics of chromosomal
1146 inversions. *Trends in Ecology & Evolution*, **33**(6), 427 – 440.
1147
1148 Wellenreuther, M., Mérot, C., Berdan, E., & Bernatchez, L. (2019). Going beyond SNPs: the role
1149 of structural genomic variants in adaptive evolution and species diversification. *Molecular*
1150 *Ecology,* **28**(6), 1203 – 1209.
1151
1152 White, M. J. D. (1978). *Modes of speciation*. W. H. Freeman, San Francisco, CA.
1153
1154 Wright, S. (1931). *Evolution in Mendelian populations*. University of Chicago, Chicago, Illinois.
1155
1156 Yada, T., & Tort, L. (2016). Stress and disease resistance: Immune system and immunoendocrine
1157 interactions. *Fish Physiology*, **35**, 365 – 403.
1158
1159 Yates, M. C., Debes, P. V., Fraser, D. J., Hutchings, J. A. (2015). The influence of hybridization
1160 with domesticated conspecifics on alternate reproductive phenotypes in male Atlantic salmon in
1161 multiple temperature regimes. *Canadian Journal of Fisheries and Aquatic Sciences*, **72**(8), 1138
1162 – 1145.
1163
1164 Yu, G., Wang, L.-G., Han, Y., & He, Q.-Y. (2012). clusterProfiler: An R package for comparing
1165 biological themes among gene clusters. *OMICS: A Journal of Integrative Biology*, **16**(5), 284–
1166 287.
1167
1168 Zhang, Y., Qin, C., Yang., L., Lu, R., Zhao, X., & Nie, G. (2018). A comparative genomics study
1169 of carbohydrate/glucose metabolic genes: from fish to mammals. *BMC Genomics*, **246**.
1170 https://doi.org/10.1186/s12864-018-4647-4.
1171
1172

1173 **AUTHOR CONTRIBUTIONS**

1174 K.B.W., S.J.L., I.R.B., and P.B. contributed to the conception and design of the study. M.K., and

1175 S.L. K.B.W., S.J.L., A.E., B.P., and T.K. performed statistical analyses. I.R.B., S.L., M.K., and

1176 S.D. provided molecular data and metadata for the study. K.B.W. drafted the manuscript and all

1177 authors contributed to the writing and approved the final draft of the manuscript.

1178

1179 **DATA ACCESSIBILITY** (data must be archived on a publicly accessible repository)

1180

1181

1182 Table 1 Sampling locations of Atlantic Salmon (*Salmo salar*) in Placentia Bay, Newfoundland,
1183 Canada. Rivers ordered geographically, east to west around the bay. Samples were collected in
1184 2017 and 2018. Number of samples genotyped (*N*) per site per year.

| River	RiverID	Longitude (∘W)	Latitude (∘N)	N_{2017}	N_{2018}
Branch River	BRA	-53.97	46.89	30	32
Lance River	LAN	-54.07	46.82	9	-
Cuslett Brook	CUS	-54.16	46.96	30	30
Great Barasway Brook	GBW	-54.06	47.13	30	41
Little Barasway Brook	LBB	-54.04	47.18	16	-
Southeast Placentia River	SPR	-53.88	47.23	30	31
Northeast Placentia River	NPR	-53.84	47.27	30	24
Ship Harbour Brook	SHI	-53.87	47.35	30	32
Fair Haven Brook	FHB	-53.89	47.54	30	30
Come By Chance River	CBC	-53.98	47.86	30	31
North Harbour River	NHR	-54.03	47.92	30	32
Black River	BLA	-54.16	47.89	30	30
Pipers Hole Brook	PHR	-54.27	47.93	30	33
Sandy Harbour River	SHA	-54.36	47.71	30	9
Nonsuch River	NON	-54.65	47.45	30	20
Cape Roger Brook	CRB	-54.69	47.44	30	32
Bay de l'Eau River	BDL	-54.73	47.51	30	32
Rushoon River	RUS	-54.92	47.37	30	37
Red Harbour East River	RHA	-54.99	47.33	30	26
Red Harbour West River	RHW	-55.01	47.29	30	30
Northwest Mortier Bay Brook	NMB	-55.31	47.17	30	32
Tides Brook	TDS	-55.26	47.13	30	28
Big Salmonier Brook	BSA	-55.22	47.06	30	31
Lawn River	LWN	-55.54	46.95	30	30
Taylor Bay Brook	TBR	-55.71	46.88	30	10
Piercey's Brook	PBR	-55.86	46.88	30	21

1185

1186

1187

1188

1189

Table 2 Summary of genetic diversity for Atlantic Salmon from 26 rivers in Placentia Bay, Newfoundland, Canada. Rivers are ordered geographically, east to west around the bay. Number of samples (N), mean observed (H_o) and expected (H_e) heterozygosity and median F_{IS} calculated across putatively neutral loci ($n = 6{,}302$) using *hierfstat*.

| RiverID | 2017 | | | | 2018 | | | |
	N	H_o	H_e	F_{IS}	N	H_o	H_e	F_{IS}
BRA	30	0.184	0.182	-0.025	32	0.187	0.183	-0.025
LAN	9	0.181	0.170	-0.067	-	-	-	-
CUS	30	0.184	0.185	-0.018	30	0.189	0.185	-0.036
GBW	18	0.188	0.186	-0.030	41	0.189	0.186	-0.026
LBB	15	0.191	0.184	-0.037	-	-	-	-
SPR	27	0.192	0.185	-0.040	30	0.194	0.188	-0.036
NPR	29	0.193	0.192	-0.018	17	0.192	0.191	-0.032
SHI	22	0.202	0.200	-0.024	32	0.204	0.201	-0.018
FHB	30	0.188	0.185	-0.036	25	0.193	0.188	-0.029
CBC	30	0.192	0.194	-0.018	19	0.194	0.192	-0.029
NHR	24	0.188	0.188	-0.022	29	0.192	0.189	-0.018
BLA	24	0.196	0.195	-0.022	29	0.198	0.198	-0.018
PHR	29	0.193	0.193	-0.018	30	0.196	0.194	-0.018
SHA	30	0.198	0.196	-0.018	9	0.197	0.198	0.000
NON	27	0.181	0.177	-0.020	20	0.181	0.180	-0.027
CRB	29	0.190	0.190	-0.018	27	0.183	0.182	-0.020
BDL	30	0.181	0.181	-0.018	32	0.188	0.187	-0.016
RUS	25	0.182	0.183	-0.021	31	0.182	0.182	-0.017
RHA	30	0.158	0.158	-0.018	26	0.159	0.158	-0.020
RHW	27	0.196	0.196	-0.020	24	0.196	0.194	-0.022
NMB	27	0.185	0.181	-0.040	31	0.193	0.189	-0.035
TDS	15	0.179	0.177	-0.037	24	0.186	0.185	-0.022
BSA	30	0.188	0.187	-0.018	24	0.187	0.184	-0.022
LWN	27	0.193	0.190	-0.020	22	0.195	0.194	-0.024
TBR	18	0.193	0.194	-0.030	10	0.192	0.199	0.000
PBR	30	0.194	0.194	-0.018	17	0.194	0.192	-0.032

1194

1195
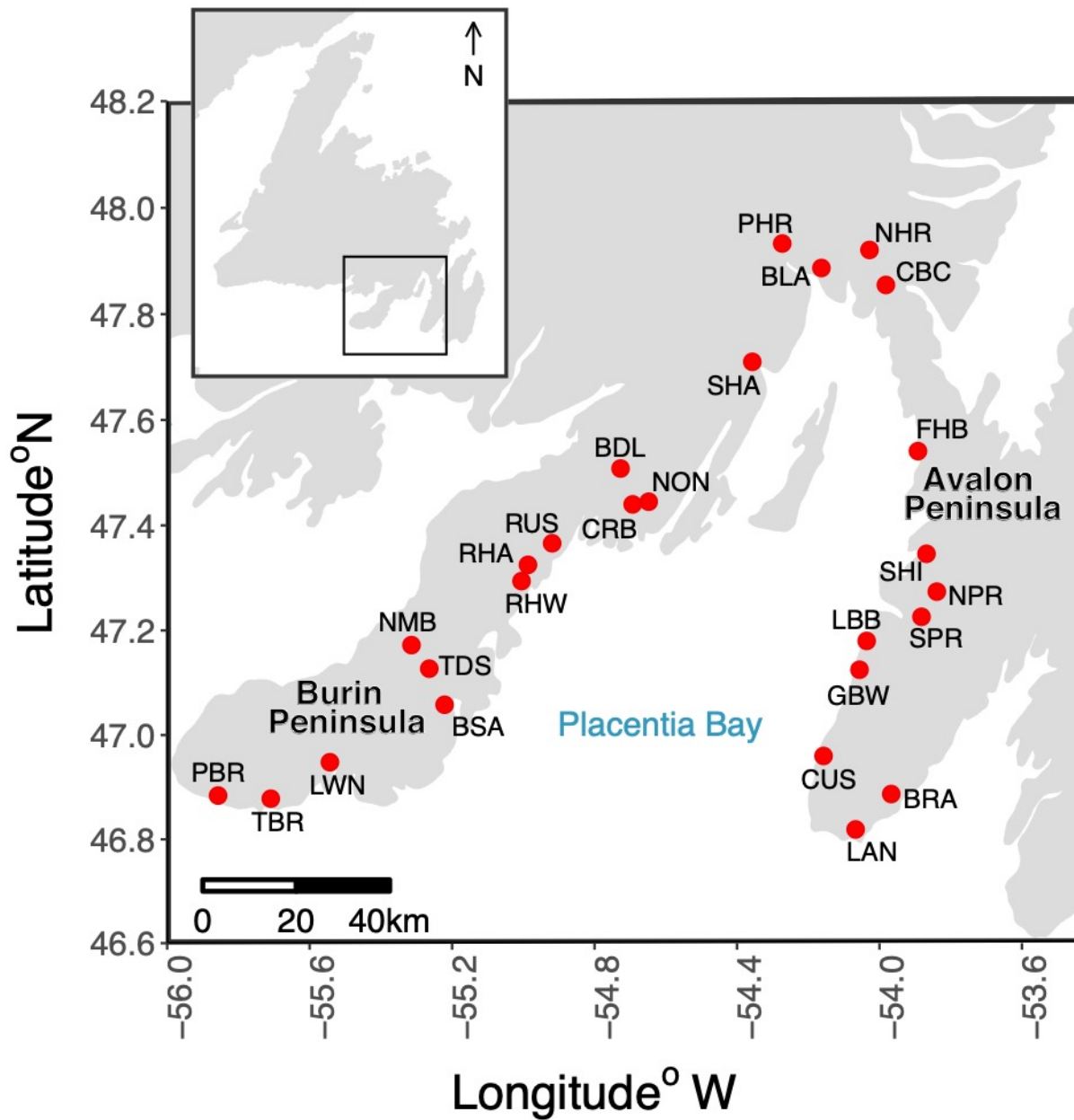
Figure 1 Sampling locations (n = 26, red circles) of juvenile Atlantic Salmon (*Salmo salar*) in Placentia Bay, Newfoundland, Canada. Samples collected in 2017 and 2018; see Table 1 for details.
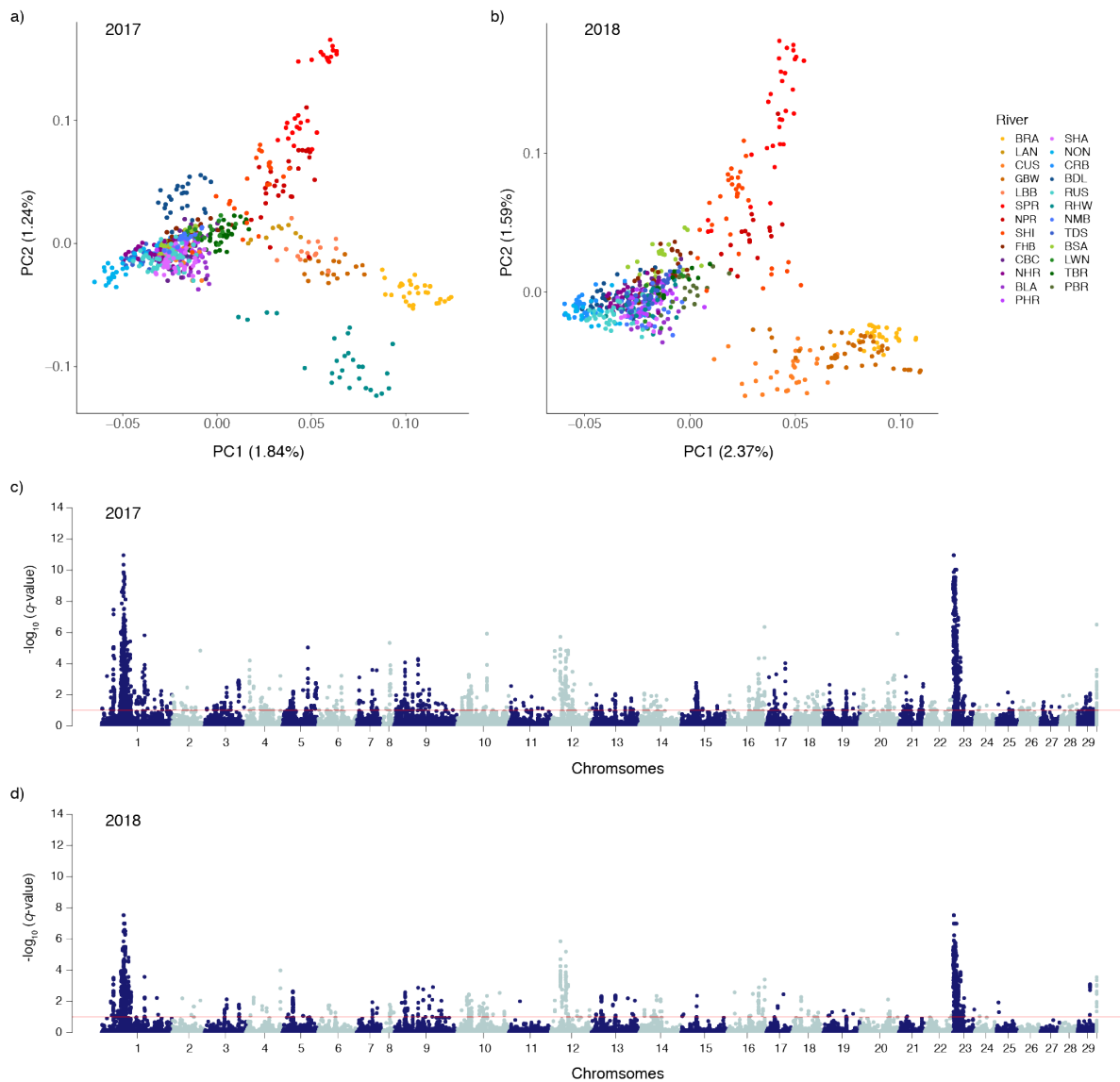
1201

Figure 2 Genomic outlier blocks drive spatial structure of Atlantic Salmon. (a, b) Genetic
structure across Placentia Bay, Newfoundland, Canada based on the first two principal
component (PC) axes from *pcadapt* (Luu et al., 2017) using 138,451 SNPs. (c, d) Manhattan
plots showing genomic regions of variation based on PC1. Samples collected in (a, c) 2017 (b, d)
2018. Rivers coloured east (yellow-red) to west (green-blue) with head of the bay (purple); see
Figure 1 and Table 1 for location details. Red line represents a genome-wide significance
threshold of 5.0e-8.

1209
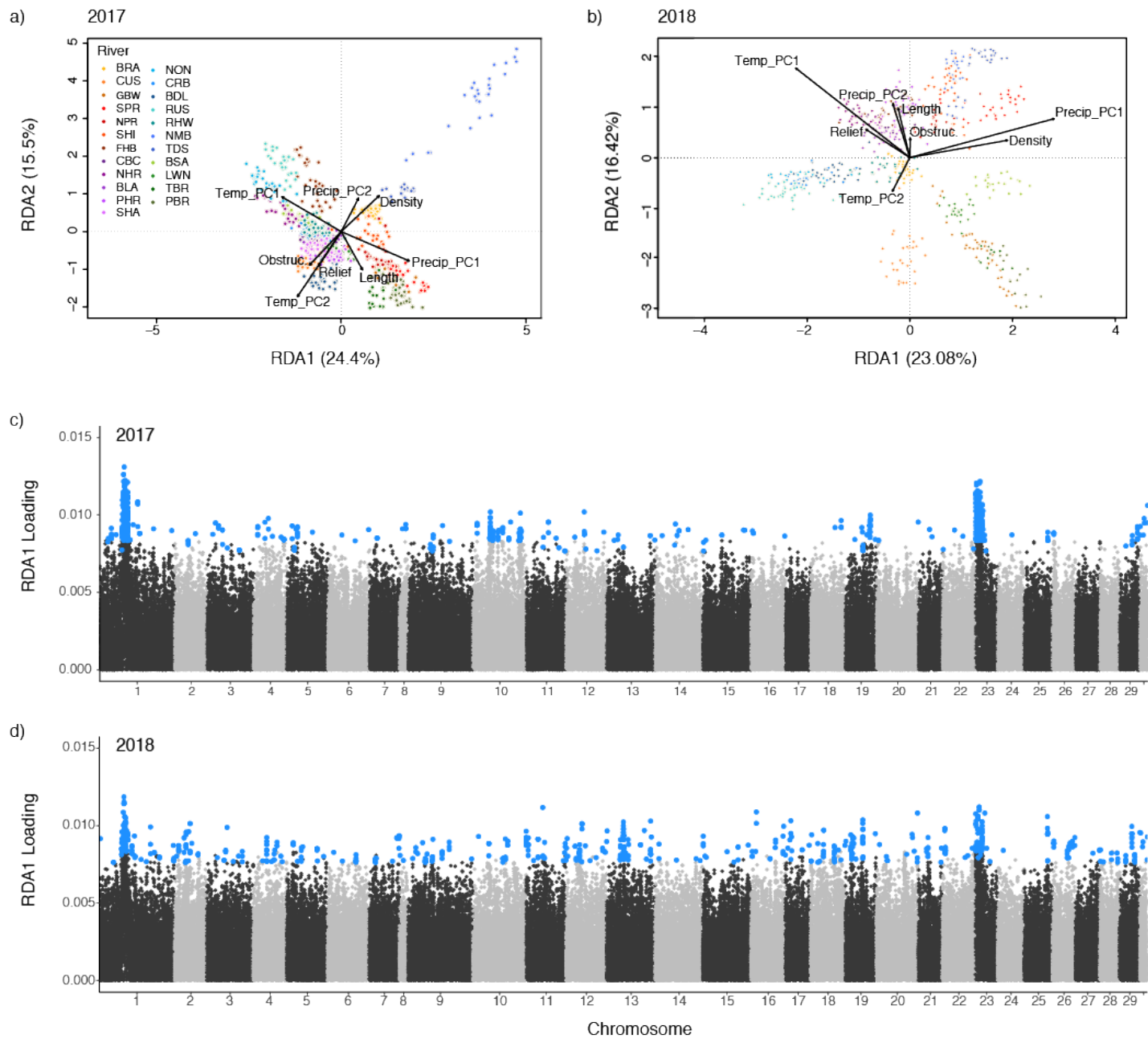
1210

Figure 3 Redundancy analysis (RDA) of (a) 2017 and (b) 2018 based on PCs 1 and 2 of BIOCLIM

(WorldClim) temperature and precipitation variables, and habitat variables. Manhattan plots,

showing absolute loadings, of the distribution of outlier SNPs (blue) associated with the first

RDA axis of (c) 2017 and (d) 2018. See Figure 1 and Table 1 for location details.

1215
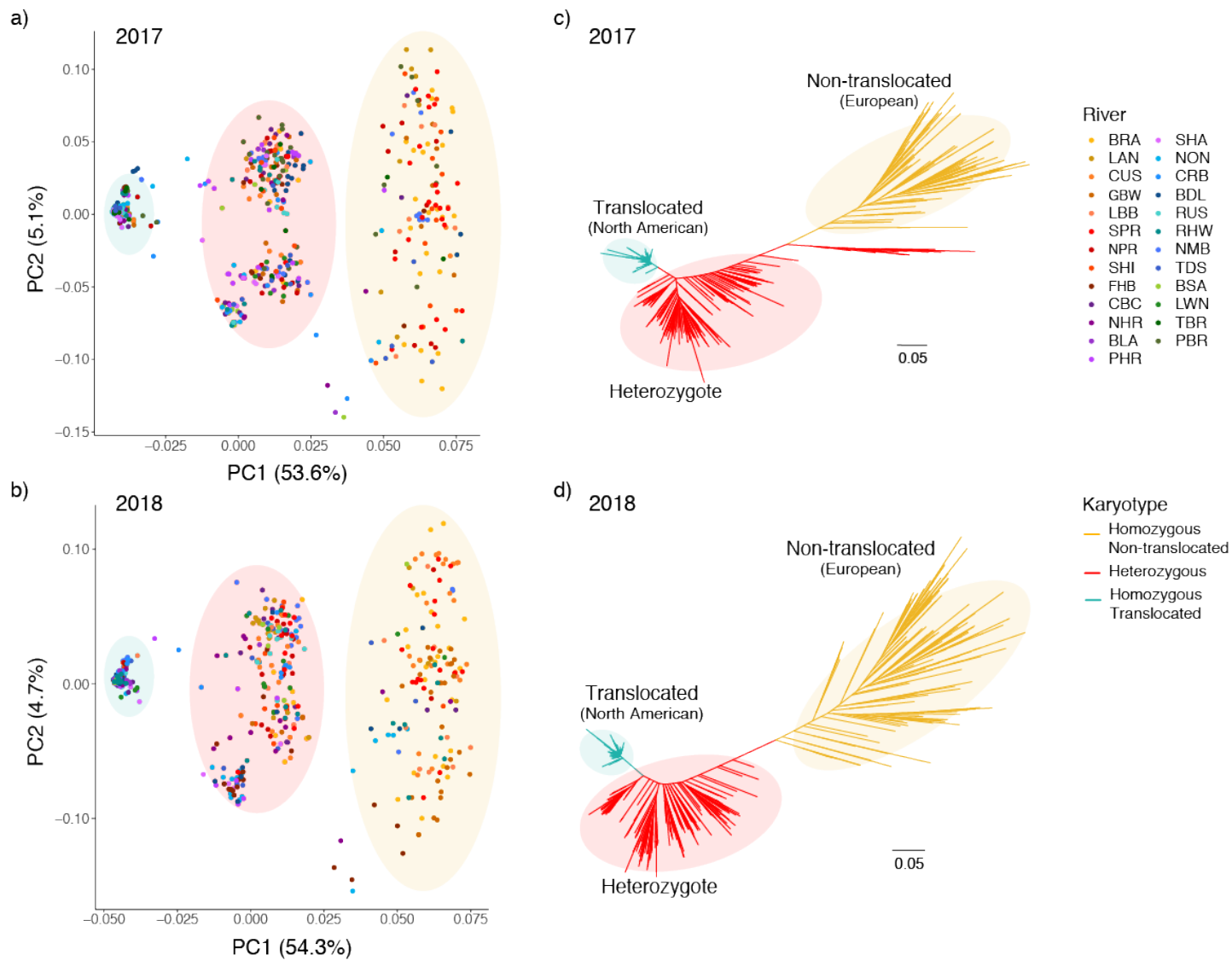
1216

Figure 4 Genetic relationships between individual Atlantic Salmon based on outlier SNPs ($q <$

0.05) within the Ssa01p/Ssa23 chromosomal translocation. Samples collected in (a) 2017 and (b)

2018. Neighbor-joining (NJ) tree for (c) 2017 and (d) 2018. Homozygous European non-

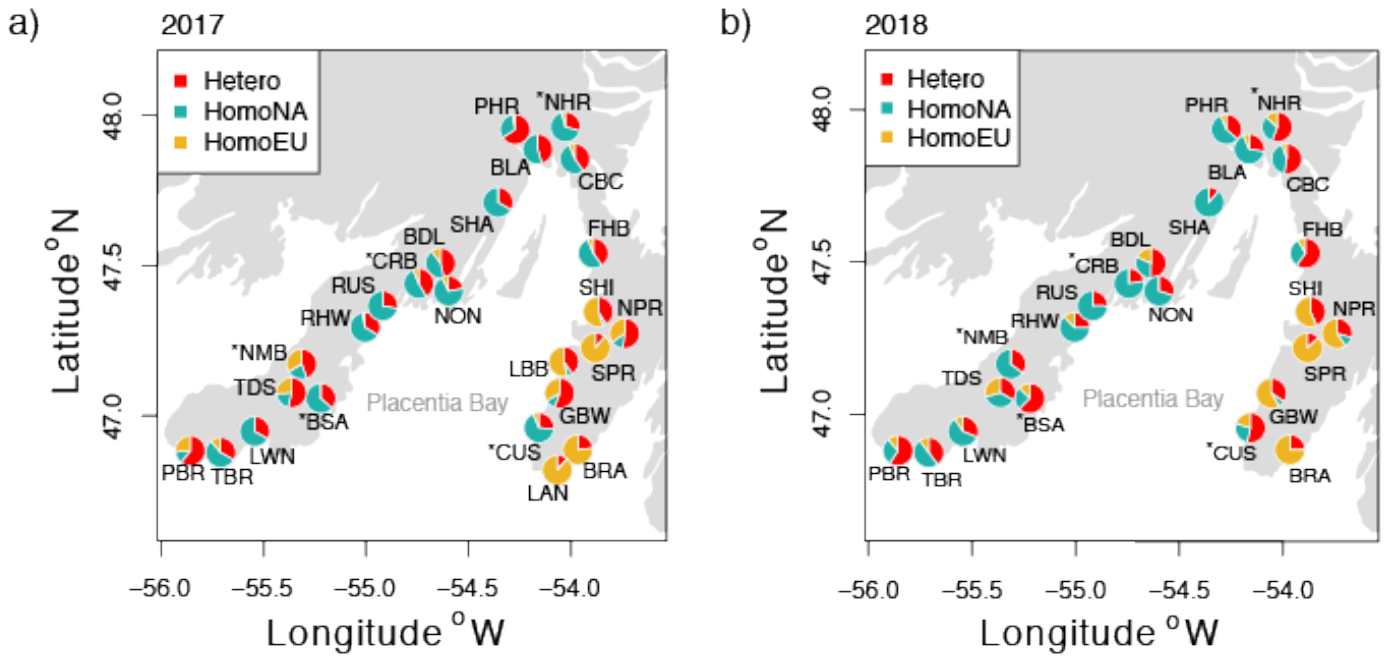translocated (Ssa01p/q and Ssa23) karyotype (yellow), heterozygous (red), and homozygous

North American translocated (Ssa01q and Ssa01p/23) karyotype (blue-green). See Figure 1 and

Table 1 for location details.

1223

1224

1225

1226 Figure 5 Frequency of Ssa01 and Ssa23 chromosomal translocation exhibits fine-scale spatial

1227 variability in Placentia Bay, Newfoundland, Canada. (a, b) Karyotype frequency within river in

1228 (a) 2017 and (b) 2018. Asterisk (*) indicates karyotype frequency differed significantly between

1229 years. (c) Translocation frequency between rivers across years. Homozygous European non-

1230 translocated (Ssa01p/q and Ssa23) karyotype (yellow), heterozygous (red), and homozygous

1231 North American translocated (Ssa01q and Ssa01p/23) karyotype (blue-green). See Table 1 for

1232 location and sample details.

1233

1234

1235

1236
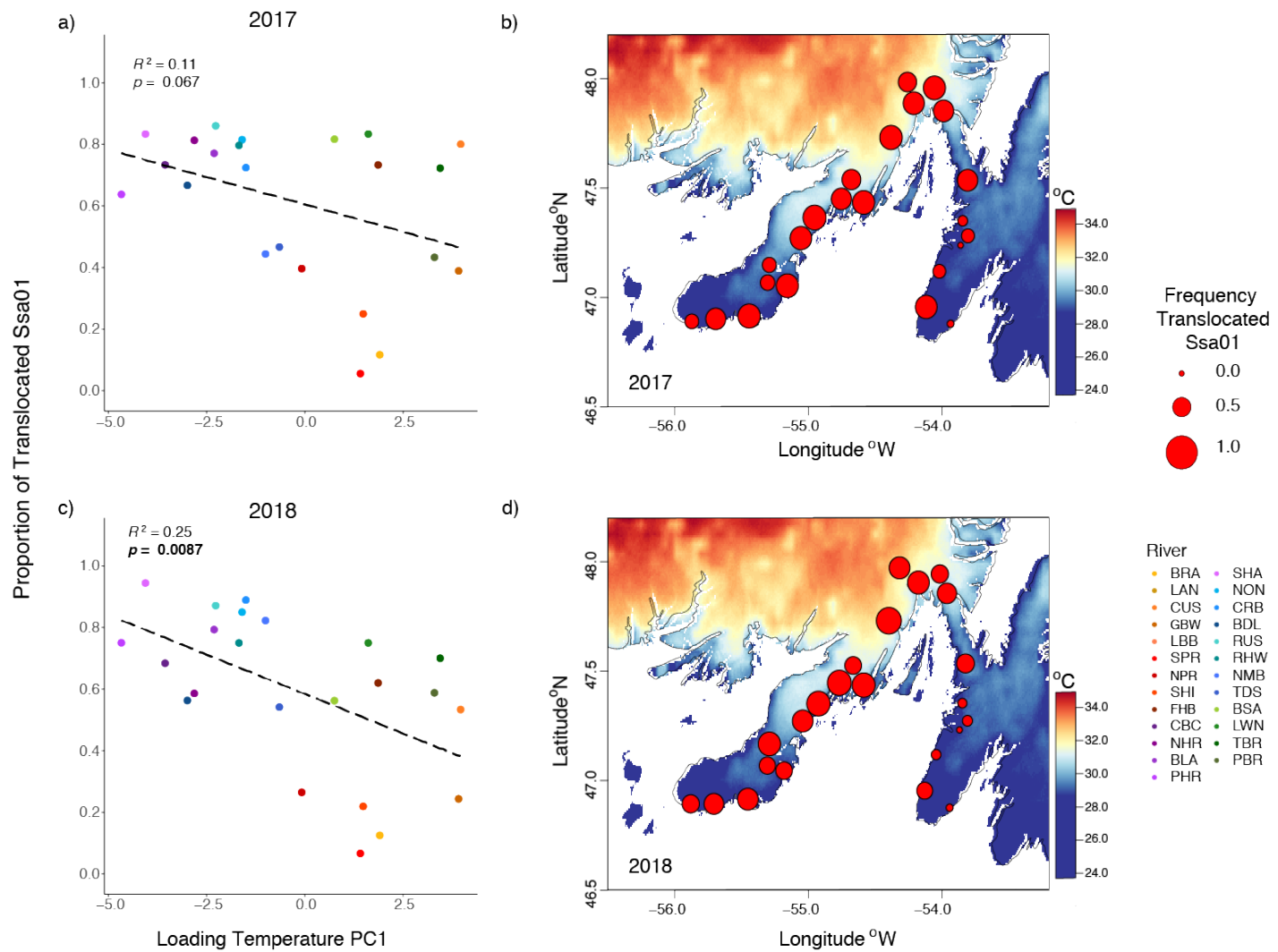
1237

Figure 6 Correlation between temperature and the Ssa01/Ssa23 chromosomal translocation in

Atlantic Salmon within Placentia Bay, Newfoundland, Canada. (a, c) Linear regression of the

first principal component (PC) of a PCA based on 11 temperature variables (BIOCLIM) and

proportion of non-translocated Ssa01p/q sampled in (a) 2017 and (c) 2018. (b, d) Temperature

annual range (BIO7), the highest loading variable on temperature PC1. Size of point indicates

frequency of non-translocated Ssa01p/q in (b) 2017 and (d) 2018. See Table 1 for location details.

1244

50

Supplemental Information

1247 Table S1 Climatic and habitat variables used to identify potential drivers of translocation

1248 frequency using a partial redundancy analysis (RDA). Description of each measure is provided

1249 with the years measured, unit, and data source.

Variable	Description	Unit	Year	Source
BIO1	Annual mean temperature	°C	1970-2000	WorldClim
BIO2	Mean diurnal range	°C	1970-2000	WorldClim
BIO3	Isothermality	°C	1970-2000	WorldClim
BIO4	Temperature seasonality	°C	1970-2000	WorldClim
BIO5	Max temperature of warmest month	°C	1970-2000	WorldClim
BIO6	Min temperature of coldest month	°C	1970-2000	WorldClim
BIO7	Temperature annual range	°C	1970-2000	WorldClim
BIO8	Mean temperature wettest quarter	°C	1970-2000	WorldClim
BIO9	Mean temperature of driest quarter	°C	1970-2000	WorldClim
BIO10	Mean temperature warmest quarter	°C	1970-2000	WorldClim
BIO11	Mean temperature coldest quarter	°C	1970-2000	WorldClim
BIO12	Annual precipitation	mm	1970-2000	WorldClim
BIO13	Precipitation of wettest month	mm	1970-2000	WorldClim
BIO14	Precipitation of driest month	mm	1970-2000	WorldClim
BIO15	Precipitation seasonality	mm	1970-2000	WorldClim
BIO16	Precipitation of wettest quarter	mm	1970-2000	WorldClim
BIO17	Precipitation of driest quarter	mm	1970-2000	WorldClim
BIO18	Precipitation of warmest quarter	mm	1970-2000	WorldClim
BIO19	Precipitation of coldest quarter	mm	1970-2000	WorldClim
Human density	Human population density		2000	NASA NEO
Axial length	Length of river along down-valley axis	km	1974	DFO
Obstructions	Number of obstructions		1974	DFO
Relief	Difference in elevation between the highest and lowest point of the basin	m	1974	DFO
FW_dem_max	Maximum elevation	m	2000	HydroSHEDS

1250

1251

1252

1253 Table S2 Outlier block regions associated with a known chromosomal translocation

1254 (Ssa01p/Ssa23) in Atlantic salmon identified here using *pcadapt* across rivers in Placentia Bay,

1255 Newfoundland, Canada. Outlier block regions were approximated by visual inspection of *q*-

1256 values. Boundaries of and number of significant (*q*-value < 0.05) single nucleotide

1257 polymorphisms (SNPs) in each region reported.

Chromosome	Approximate boundaries of outlier blocks		Number of outlier SNPs
	Start (bp)	End (bp)	
Ssa01	44,000,000	53,000,000	480
Ssa23	0	9,500,000	407

1258

1259

1260

1261

1262

1263

1264

1265

1266

1267

1268

1269

1270

1271

1272

1273   Table S3 Principal component, PC1 and PC2, loadings for each categorical PCA used in

1274   redundancy analyses (RDA) with code of climatic variable.

Climatic variable	Loading	
	PC1	PC2
Temperature		
BIO1	-0.19	-0.62
BIO2	0.34	-0.11
BIO3	0.20	-0.26
BIO4	0.36	-0.013
BIO5	0.34	-0.078
BIO6	-0.36	-0.036
BIO7	0.36	0.001
BIO8	-0.17	-0.54
BIO9	0.25	-0.23
BIO10	0.30	-0.38
BIO11	-0.35	-0.2
Precipitation		
BIO12	-0.39	0.048
BIO13	-0.38	0.18
BIO14	-0.37	-0.20
BIO15	-0.17	0.81
BIO16	-0.38	0.19
BIO17	-0.35	-0.42
BIO18	-0.37	-0.24
BIO19	-0.37	0.01

1275

1276

1277

1278

1279

1280

1282 Table S4 Proportion of karyotypes for the Ssa01p/Ssa23 chromosomal translocation in Placentia

1283 Bay, Newfoundland, Canada. Karyotype assigned based on outlier SNPs ($n = 887$) from the

1284 outlier block regions on Ssa01p and Ssa23. Rivers are ordered geographically, east to west

1285 around the bay. See Figure 1 and Table 1 for location details.

	2017			2018		
RiverID	**Homo NA (Trans)**	**Hetero**	**Homo EU (No Trans)**	**Homo NA (Trans)**	**Hetero**	**Homo EU (No Trans)**
BRA	0.000	0.233	0.767	0.000	0.250	0.750
CUS	0.667	0.267	0.067	0.267	0.533	0.200
GBW	0.111	0.556	0.333	0.073	0.341	0.585
SPR	0.000	0.111	0.889	0.000	0.133	0.867
NPR	0.138	0.517	0.345	0.118	0.294	0.588
SHI	0.045	0.409	0.545	0.000	0.438	0.563
FHB	0.533	0.400	0.067	0.320	0.600	0.080
CBC	0.533	0.400	0.067	0.421	0.526	0.053
NHR	0.667	0.292	0.042	0.310	0.552	0.138
BLA	0.542	0.458	0.000	0.655	0.276	0.069
PHR	0.310	0.655	0.034	0.567	0.367	0.067
SHA	0.667	0.333	0.000	0.889	0.111	0.000
NON	0.704	0.222	0.074	0.700	0.300	0.000
CRB	0.517	0.414	0.069	0.778	0.222	0.000
BDL	0.433	0.467	0.100	0.313	0.500	0.188
RUS	0.720	0.280	0.000	0.742	0.258	0.000
RHW	0.630	0.333	0.037	0.625	0.250	0.125
NMB	0.222	0.444	0.333	0.645	0.355	0.000
TDS	0.200	0.533	0.267	0.375	0.333	0.292
BSA	0.633	0.367	0.000	0.250	0.625	0.125
LWN	0.667	0.333	0.000	0.591	0.318	0.091
TBR	0.556	0.333	0.111	0.500	0.400	0.100
PBR	0.133	0.600	0.267	0.294	0.588	0.118

1286

1287

1288

1289 Table S5 Pairwise comparison of translocation and karyotype frequencies within river between

1290 years (2017 and 2018) sampled. Bold *p*-values indicate significantly different frequencies,

1291 calculated using a Fisher Exact Test. Rivers ordered geographically, east to west, around

1292 Placentia Bay, Newfoundland; see Figure 1 and Table 1 for location details.

RiverID	Translocation frequency				Karyotype frequency			
	Estimate	lower CI	upper CI	*p*	Estimate	lower CI	upper CI	*p*
BRA	1.08	0.32	3.77	1.00	0.00	0.00	Inf	1.00
CUS	0.29	0.12	0.69	**0.00**	7.04	0.99	85.86	**0.04**
GBW	0.51	0.20	1.29	0.13	2.58	0.18	28.50	0.57
SPR	1.21	0.19	8.68	1.00	0.00	0.00	Inf	1.00
NPR	0.55	0.19	1.50	0.26	1.95	0.22	26.24	0.65
SHI	0.84	0.31	2.32	0.82	Inf	0.04	Inf	0.42
FHB	0.60	0.24	1.44	0.22	1.95	0.12	31.65	0.60
CBC	0.79	0.30	2.14	0.65	1.00	0.02	22.06	1.00
NHR	0.33	0.12	0.86	**0.02**	6.66	0.55	370.64	0.14
BLA	1.14	0.40	3.18	0.82	Inf	0.12	Inf	0.51
PHR	1.69	0.72	4.08	0.23	1.06	0.05	69.29	1.00
SHA	3.36	0.42	156.00	0.44	0.00	0.00	Inf	1.00
BDL	0.65	0.29	1.42	0.27	2.52	0.41	19.57	0.43
NON	1.28	0.38	4.75	0.78	0.00	0.00	8.01	0.51
CRB	3.02	1.01	10.31	**0.03**	0.00	0.00	4.25	0.19
RUS	1.10	0.31	3.78	1.00	0.00	0.00	Inf	1.00
RHW	0.77	0.27	2.16	0.64	3.29	0.24	188.57	0.60
NMB	5.70	2.32	14.89	**0.00**	0.00	0.00	0.22	**0.00**
TDS	1.35	0.49	3.73	0.64	0.60	0.06	4.89	0.67
BSA	0.29	0.11	0.74	**0.01**	Inf	0.99	Inf	**0.03**
LWN	0.60	0.20	1.81	0.33	Inf	0.23	Inf	0.20
TBR	0.90	0.23	3.68	1.00	1.00	0.01	23.98	1.00
PBR	1.86	0.73	4.80	0.20	0.22	0.01	2.11	0.17

1293

1294

1295

1296

1297 Table S6 Gene ontology (GO) enrichment, using topGO, for single nucleotide polymorphisms

1298 (SNPs) identified as outliers in a genotype-environment analysis (redundancy analysis; RDA)

1299 and located within the outlier block regions on chromosomes Ssa01 and Ssa23. GO IDs in bold

1300 indicate the term was significant (p-value < 0.01) in both discrete years sampled.

GO ID	Description	2017				2018			
		N_{anno}	N_{sig}	N_{exp}	p-value	N_{anno}	N_{sig}	N_{exp}	p-value
GO:0045887	positive regulation of synaptic growth at neuromuscular junction	19	3	0.13	0.0003	19	3	0.12	0.00
GO:2000541	positive regulation of protein geranylgeranylation	6	2	0.040	0.0007	6	2	0.04	0.00
GO:0008380	RNA splicing	747	9	5.05	0.0016	747	9	4.8	0.0013
GO:0006729	tetrahydrobiopterin biosynthetic process	9	2	0.060	0.0016	9	2	0.06	0.0014
GO:0045075	regulation of interleukin-12 biosynthetic process	28	4	0.19	0.0002	28	3	0.18	0.0046
GO:0007346	regulation of mitotic cell cycle	1292	18	8.74	0.0028	1292	18	8.31	0.0023
GO:0031622	positive regulation of fever generation	12	2	0.080	0.0029	12	2	0.08	0.0026
GO:0031394	positive regulation of prostaglandin biosynthetic process	12	2	0.080	0.0029	12	2	0.08	0.0026
GO:0021912	regulation of transcription from RNA polymerase II promoter involved in spinal cord motor neuron fate specification	13	2	0.090	0.0034	13	2	0.08	0.0031

GO ID	Description								
GO:0006979	response to oxidative stress	1072	13	7.25	0.0043	1072	13	6.89	0.0032
GO:0002091	negative regulation of receptor internalization	15	2	0.10	0.0045	15	2	0.1	0.0041
GO:1900025	negative regulation of substrate adhesion-dependent cell spreading	16	2	0.11	0.0051	16	2	0.1	0.0047
GO:0021913	regulation of transcription from RNA polymerase II promoter involved in ventral spinal cord interneuron specification	19	2	0.13	0.0072	13	2	0.08	0.0031
GO:0008152	metabolic process	19535	141	132.10	0.0022	19535	134	125.64	0.0084
GO:0014850	response to muscle activity	53	3	0.36	0.0056	53	3	0.34	0.0048
GO:0048515	spermatid differentiation	330	4	2.23	0.0007	330	3	2.12	0.0122
GO:0090076	relaxation of skeletal muscle	18	2	0.12	0.0065	18	2	0.12	0.0059
GO:0034612	response to tumor necrosis factor	321	7	2.17	0.0079	321	7	2.06	0.0069
GO:0071603	endothelial cell-cell adhesion	20	2	0.14	0.0080	20	2	0.13	0.0072
GO:0046326	positive regulation of glucose import	140	5	0.95	0.0027	140	4	0.9	0.0129
GO:0043201	response to leucine	20	2	0.14	0.0080	20	2	0.13	0.0072
GO:1900028	negative regulation of ruffle assembly	21	2	0.14	0.0088	21	2	0.14	0.008
GO:0010629	negative regulation of gene expression	4286	35	28.98	0.0104	4286	35	27.57	0.0079
GO:0032496	response to lipopolysaccharide	727	10	4.92	0.0053	727	9	4.68	0.0135
GO:0048535	lymph node development	65	3	0.44	0.0098	65	3	0.42	0.0085

GO:0071340	skeletal muscle acetylcholine-gated channel clustering	23	2	0.16	0.0105	23	2	0.15	0.0095
GO:0021918	regulation of transcription from RNA polymerase II promoter involved in somatic motor neuron fate commitment	7	1	0.050	0.0464	13	2	0.08	0.0031
GO:0048378	regulation of lateral mesodermal cell fate specification	12	2	0.080	0.0029	12	1	0.08	0.0745
GO:0003256	regulation of transcription from RNA polymerase II promoter involved in myocardial precursor cell differentiation	39	1	0.26	1.0000	13	2	0.08	0.0031
GO:1901213	regulation of transcription from RNA polymerase II promoter involved in heart development	62	1	0.42	1.0000	13	2	0.08	0.0031
GO:0000430	regulation of transcription from RNA polymerase II promoter by glucose	8	0	0.050	1.0000	13	2	0.08	0.0031
GO:0000431	regulation of transcription from RNA polymerase II promoter by galactose	8	0	0.050	1.0000	13	2	0.08	0.0031
GO:0010767	regulation of transcription from RNA polymerase II promoter in response to UV-induced DNA damage	5	0	0.030	1.0000	13	2	0.08	0.0031

GO:0021882	regulation of transcription from RNA polymerase II promoter involved in forebrain neuron fate commitment	9	0	0.060	1.0000	13	2	0.08	0.0031
GO:0021920	regulation of transcription from RNA polymerase II promoter involved in spinal cord association neuron specification	5	0	0.030	1.0000	13	2	0.08	0.0031
GO:0043618	regulation of transcription from RNA polymerase II promoter in response to stress	115	0	0.78	1.0000	13	2	0.08	0.0031
GO:0043619	regulation of transcription from RNA polymerase II promoter in response to oxidative stress	36	0	0.24	1.0000	13	2	0.08	0.0031
GO:0061418	regulation of transcription from RNA polymerase II promoter in response to hypoxia	74	0	0.50	1.0000	13	2	0.08	0.0031
GO:1900094	regulation of transcription from RNA polymerase II promoter involved in determination of left/right symmetry	38	0	0.26	1.0000	13	2	0.08	0.0031
GO:0046060	dATP metabolic process	19	2	0.13	0.0072	19	0	0.12	1

1301

1302

1303

1304
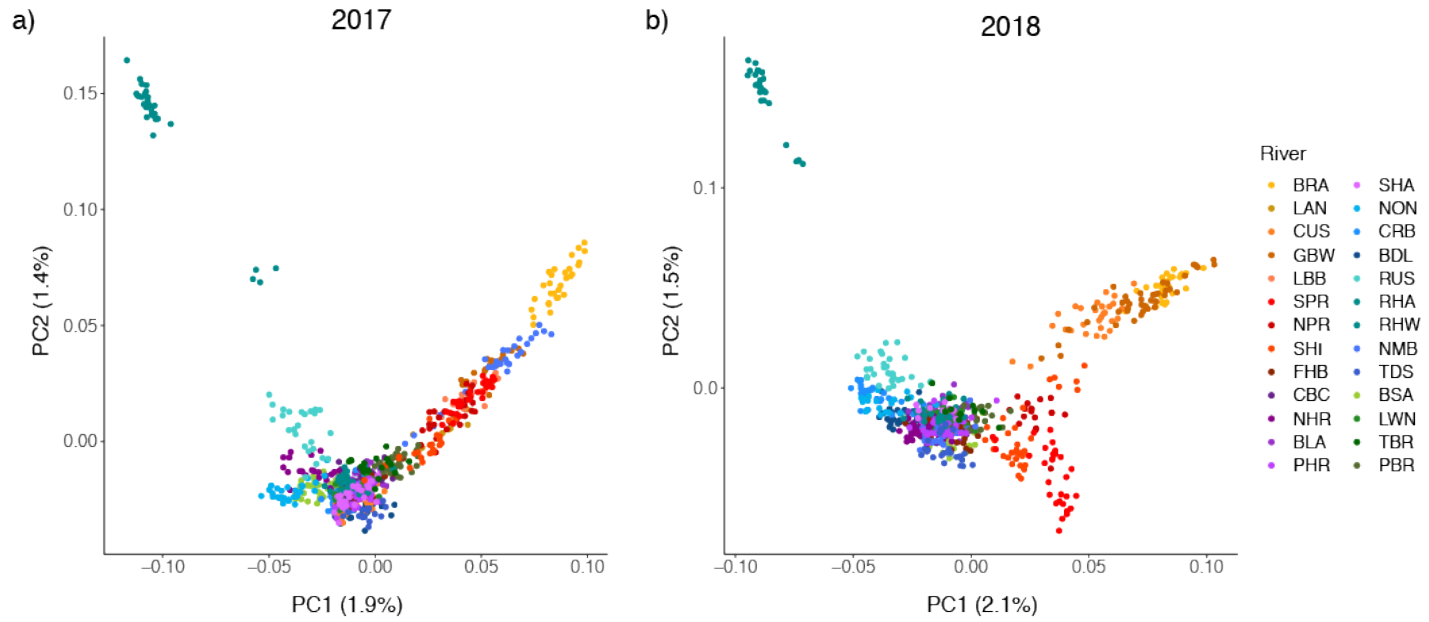
1305

1306   Figure S1 Population structure of Atlantic Salmon in Placentia Bay, Newfoundland in (a) 2017

1307   and (b) 2018. Red Harbour East (RHA) was found to be genetically differentiated from all other

1308   rivers sampled based on the first two principal component (PC) axes from *pcadapt* (Luu et al.,

1309   2017) using 139,038 SNPs. Rivers coloured east (yellow-red) to west (green-blue) with head of

1310   the bay (purple). See Figure 1 and Table 1 for location details.

1311

1312
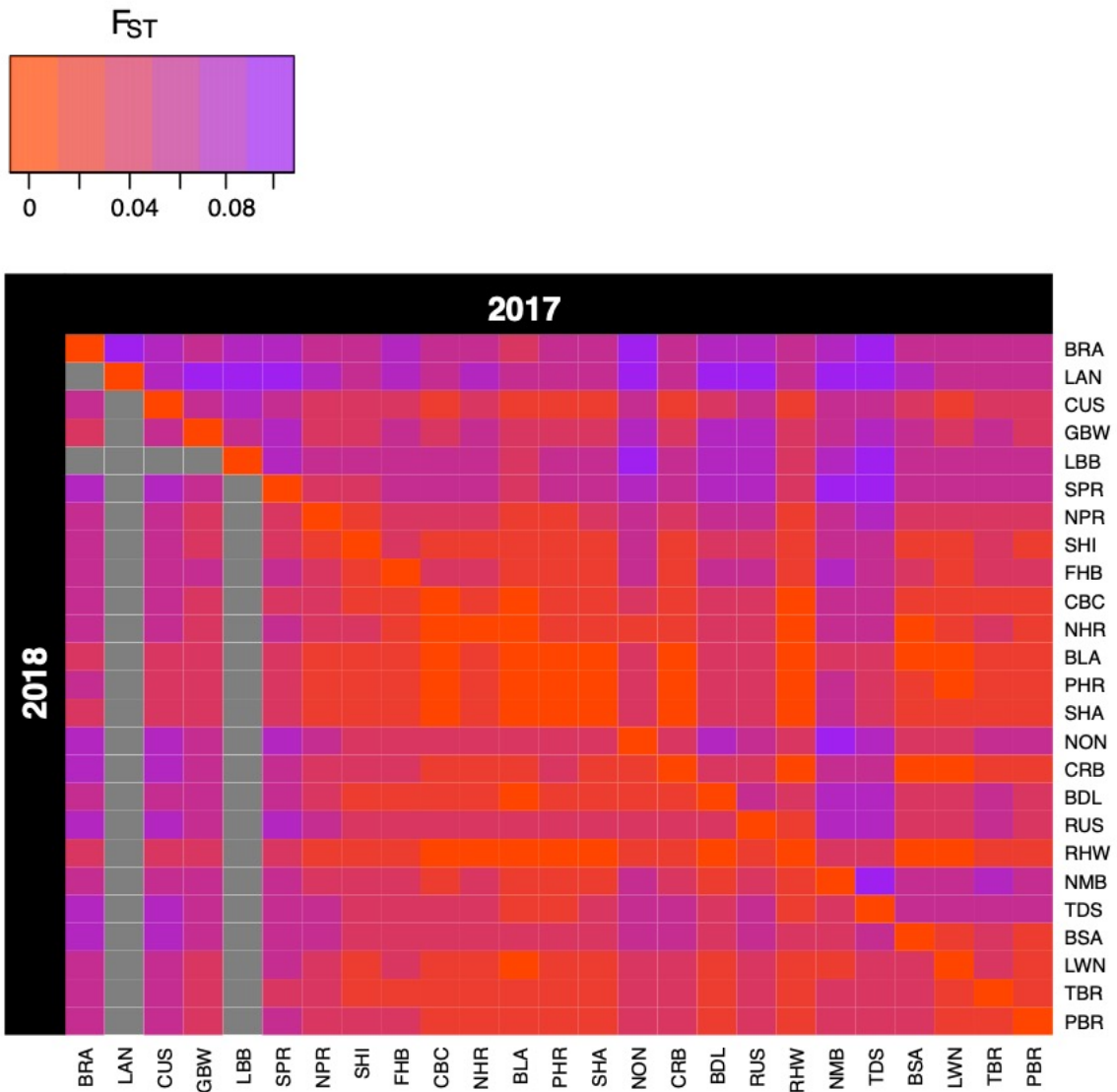
Figure S2 Heatmap of pairwise F_{ST} for Atlantic Salmon rivers ($n = 25$) in Placentia Bay, Newfoundland, Canada. The upper matrix represents 2017 and the lower matrix 2018. Rivers are ordered geographically from east to west. Lance (LAN) and Little Barasway (LBB) were not sampled in 2018. See Figure 1 and Table 1 for location details.
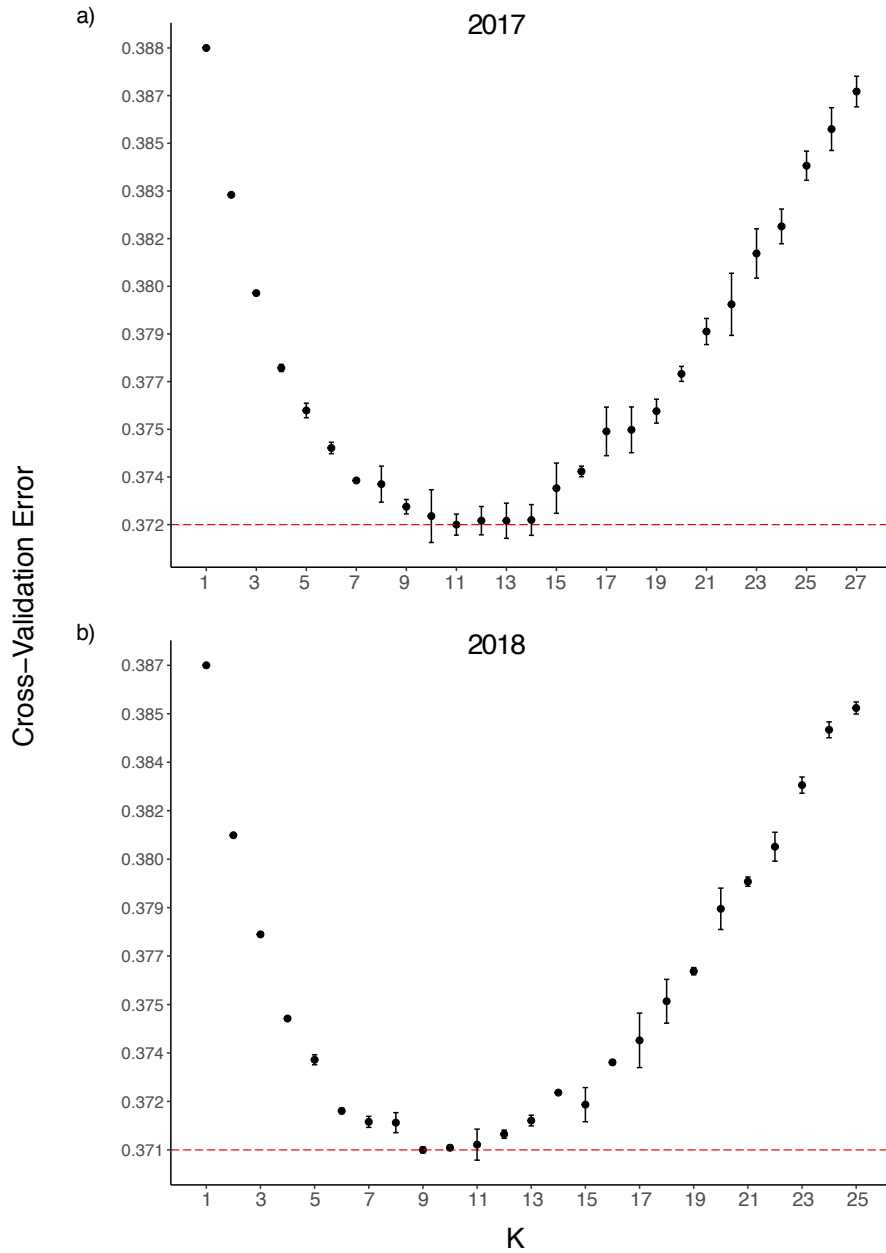
Figure S3 Cross-validation (CV) error means and standard deviations from three ADMIXTURE
runs using different random number seeds. Standard deviations which overlap the dashed red
line, indicating lowest mean CV error represent a reasonable range of K. (a) 2017, K = 10
through K = 14 and (b) 2018, K = 9 through K = 11.

1325
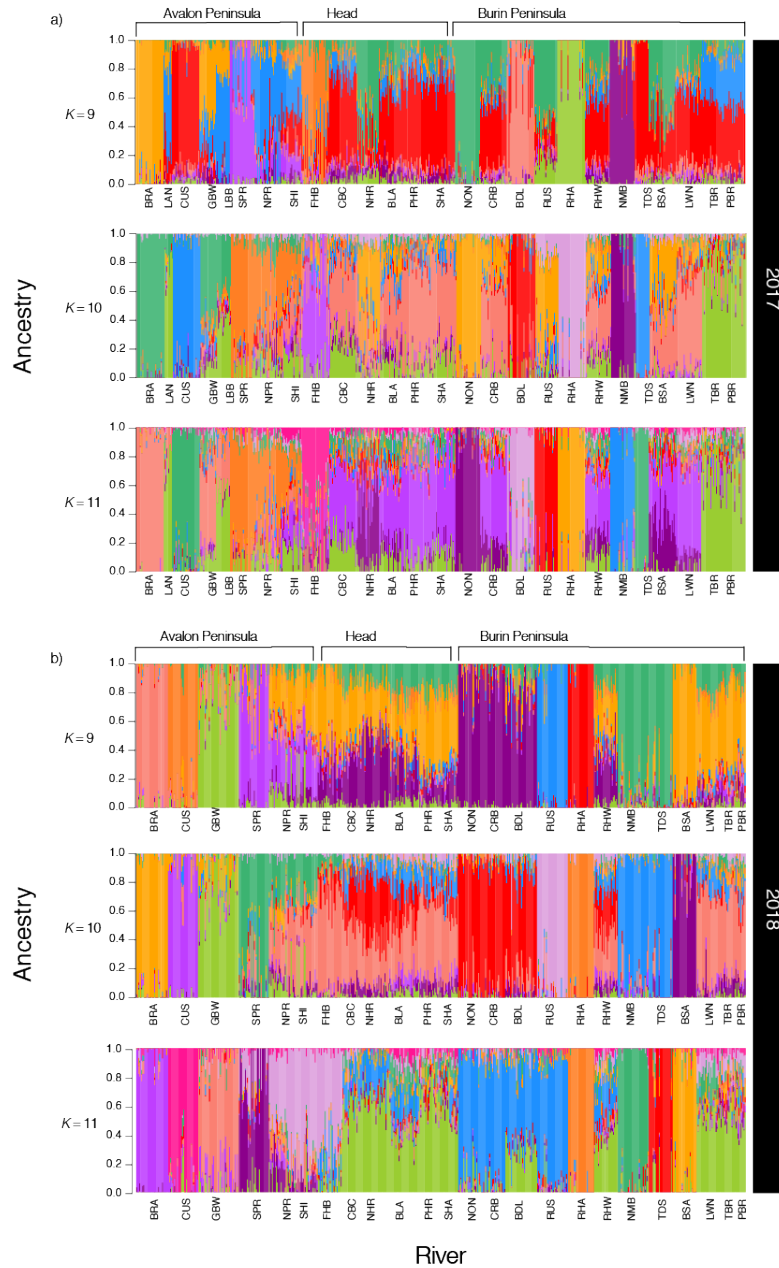
1326

Figure S4 ADMIXTURE (K = 9 – 11) results for Atlantic Salmon (*Salmo salar*) sampled in

Placentia Bay, Newfoundland, Canada in (a) 2017 (*n* = 662) and (b) 2018 (*n* = 611). Rivers

ordered geographically, east to west, around the bay; see Figure 1 and Table 1. Lance (LAN) and

Little Barasway (LBB) were not sampled in 2018 due to limited sample size in 2017.

1331
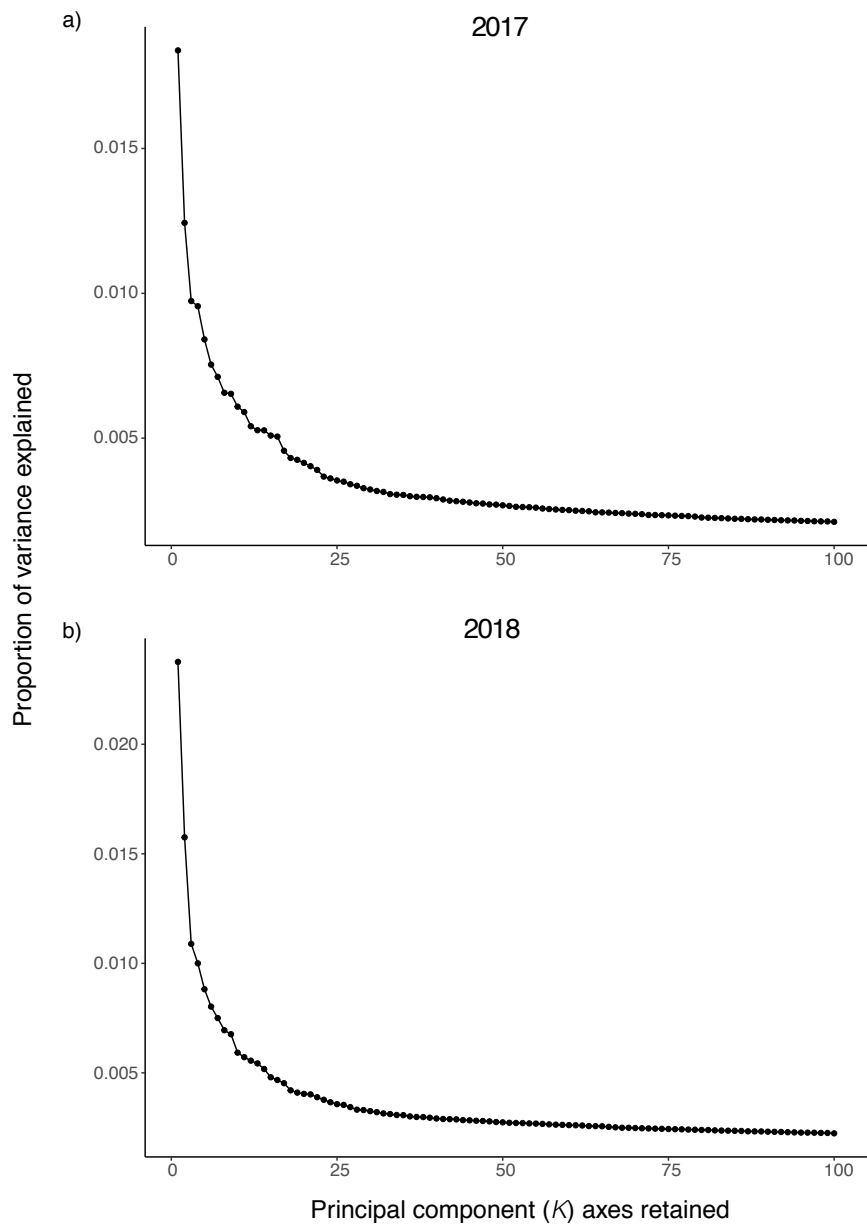
Figure S5 Scree plots generated in *pcadapt* showing proportion of variance explained as

increasing principal component (*K*) axes are retained for a) 2017 and b) 2018. Results represent

genetic variation in Atlantic Salmon (*Salmo salar*) across Placentia Bay, Newfoundland, Canada.

1332

1333

1334

1335

1336

1337

a) Homozgous Non-translocated vs. Heterozygous

b) Homozgous Translocated vs. Heterozygous

c) Homozgous Non-translocated vs. Homozygous Translocated
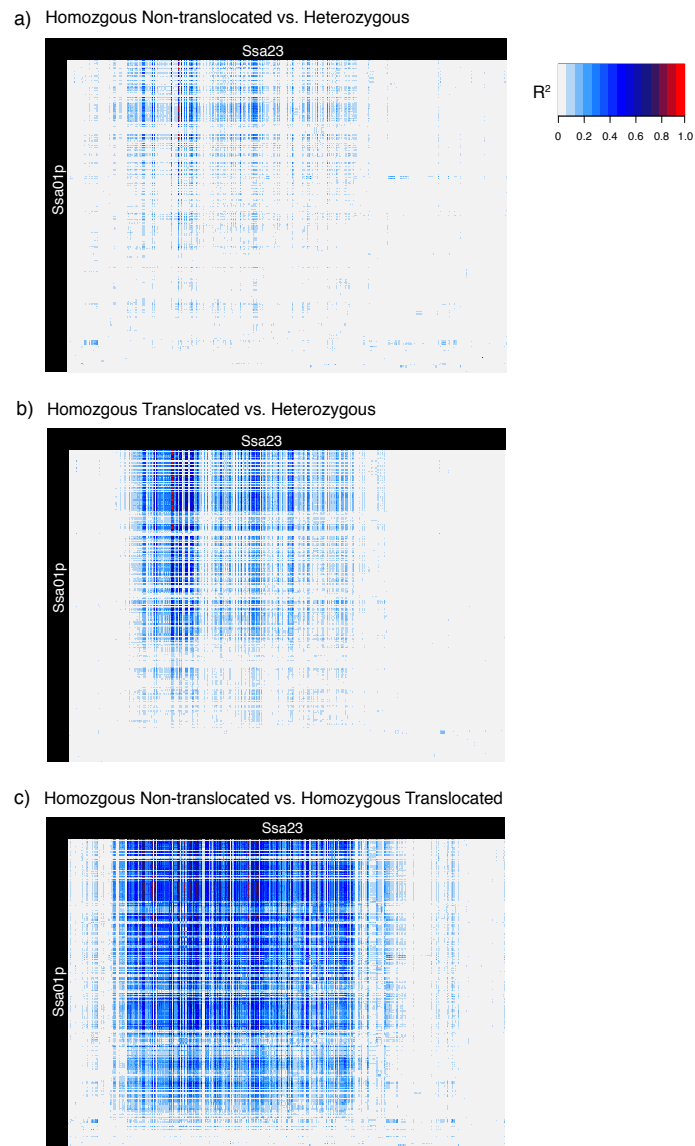
1338

Figure S6 Heatmap of linkage disequilibrium (LD) between outlier SNPs (n = 1913) within

outlier block regions on chromosomes (Ssa01p and Ssa23). Pairwise LD (R^2) for (a) homozygous

non-translocated vs. heterozygous, (b) homozygous translocated vs. heterozygous, and (c)

homozygous non-translocated vs. homozygous translocated in 2017.

1343
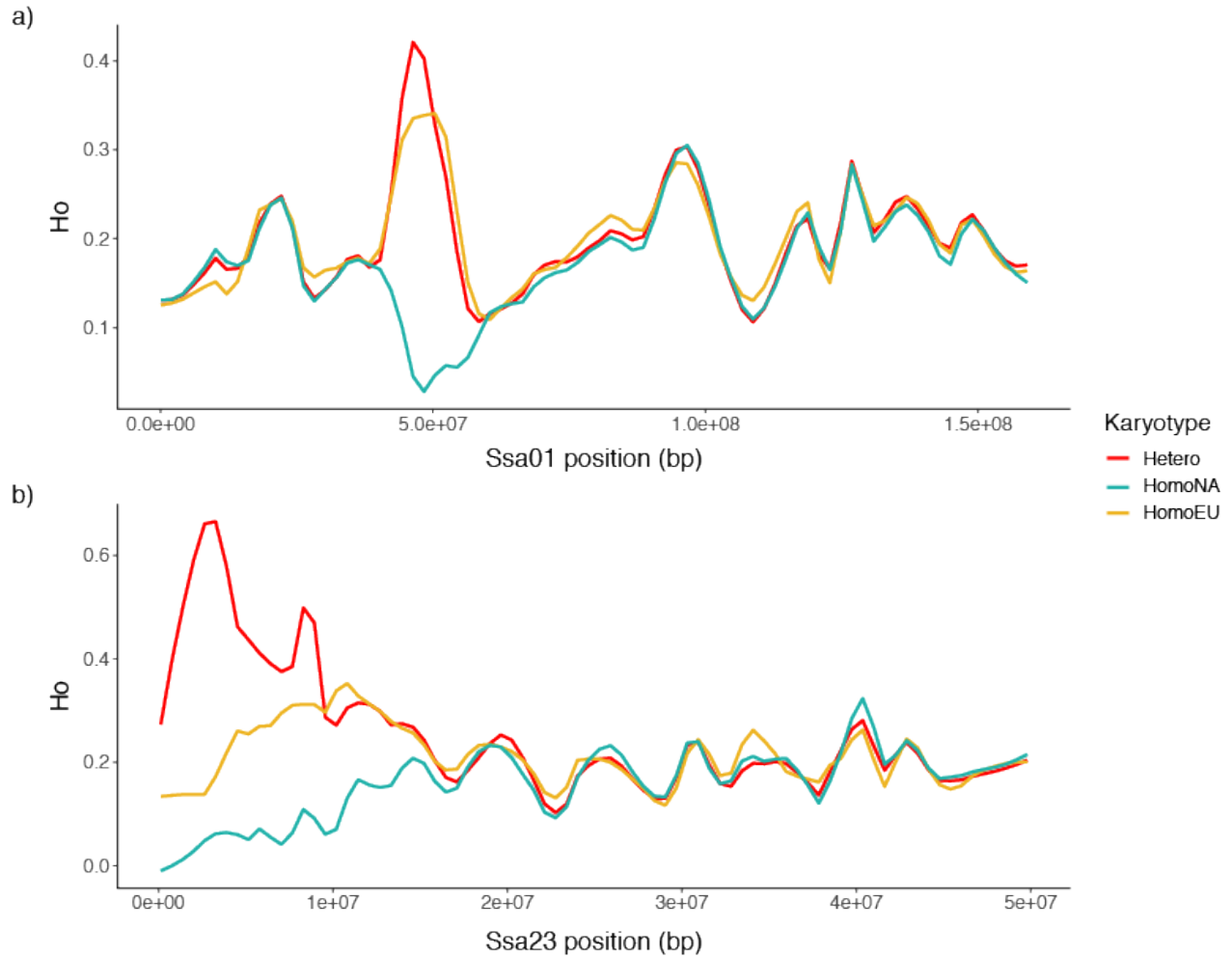
1344

1345 Figure S7 Observed heterozygosity (*H*o) for each karyotype. Karyotypes assigned using *kmeans*

1346 for three clusters; standard European (homozygous non-translocated; Ssa01p/q and Ssa23),

1347 standard North American (homozygous translocated; Ssa01p/Ssa23 and Ssa01q), and

1348 heterozygous. All values calculated in plink v1.9. Lines represent smoothed values for a span of

1349 0.1 using ggplot2.

1350

1351

1352

1353

1354
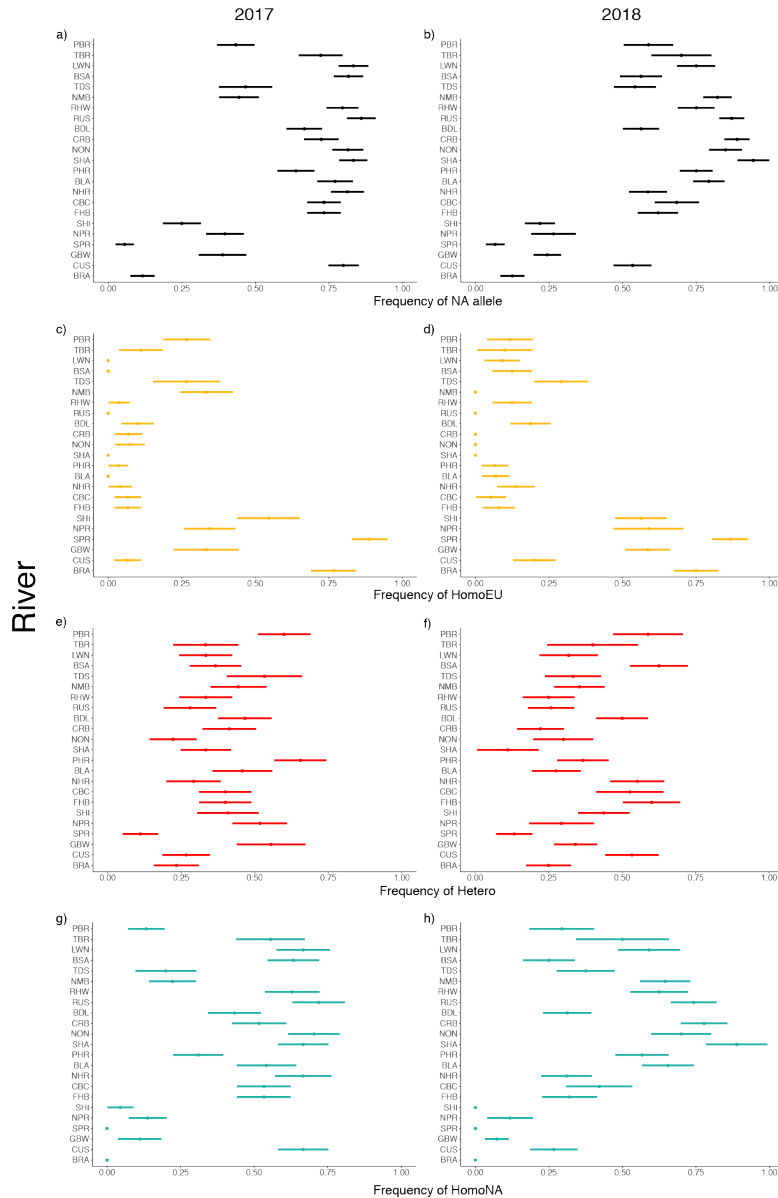
Figure S8 Heterogeneity of (a, b) translocation (c - h) and karyotype frequencies between rivers

within year, (a, c, e, and g) 2017 and (b, d, f, and h) 2018 sampled. Bars represent confidence

intervals. Rivers ordered geographically, east to west, around Placentia Bay, Newfoundland; see

Figure 1 and Table 1 for location details.. Colours indicate karyotype; homozygous non-

translocated (yellow), heterozygous (red), and homozygous translocated (blue-green).
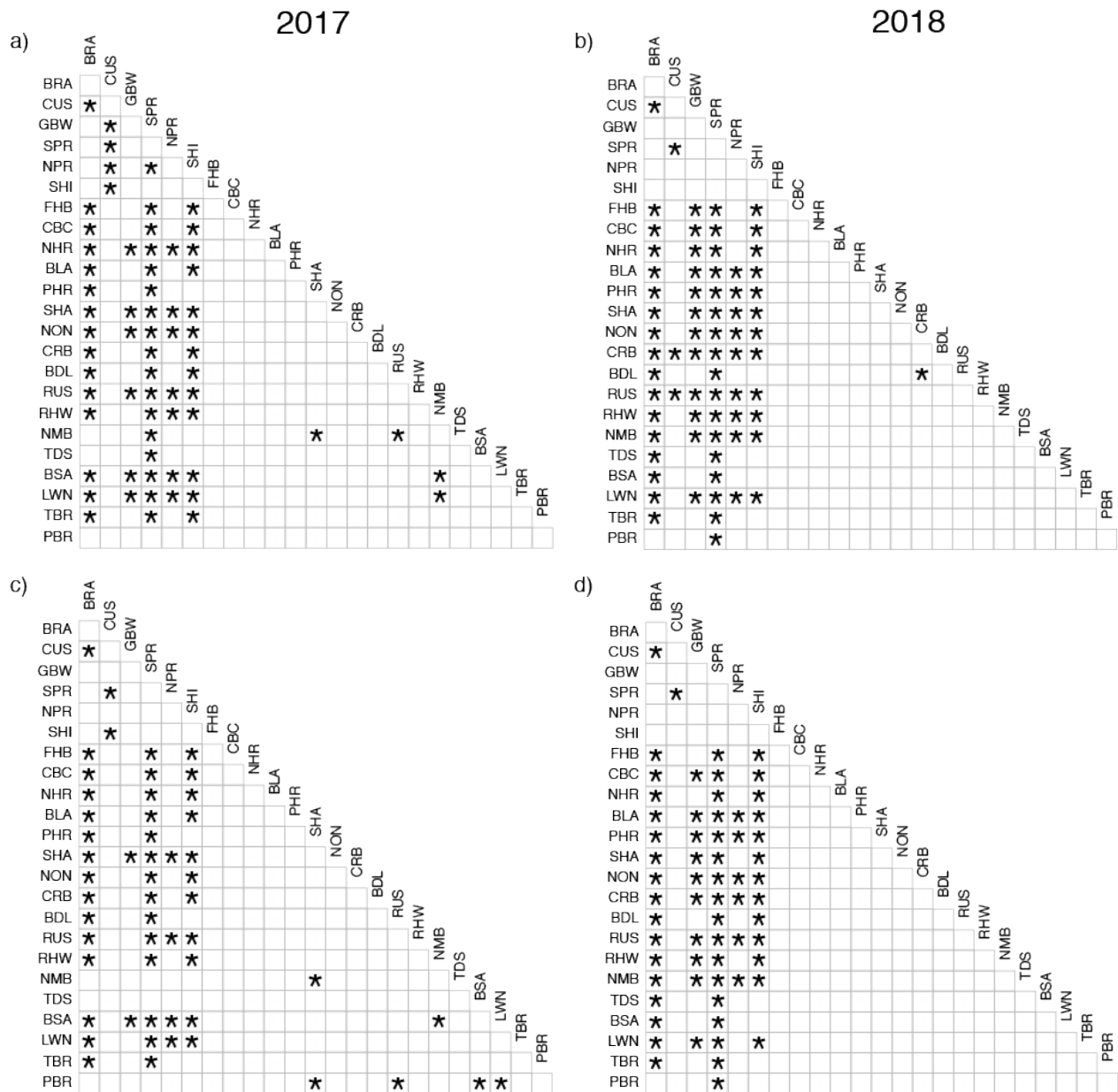
Figure S9 Pairwise comparison of (a, b) translocation (c, d) and karyotype frequencies between rivers within year, (a, c) 2017 (b, d) and 2018 sampled. Stars indicate significantly different frequencies, calculated using a Fisher Exact Test adjusted for multiple comparisons. Rivers ordered geographically, east to west, around Placentia Bay, Newfoundland; see Figure 1 and Table 1 for location details.
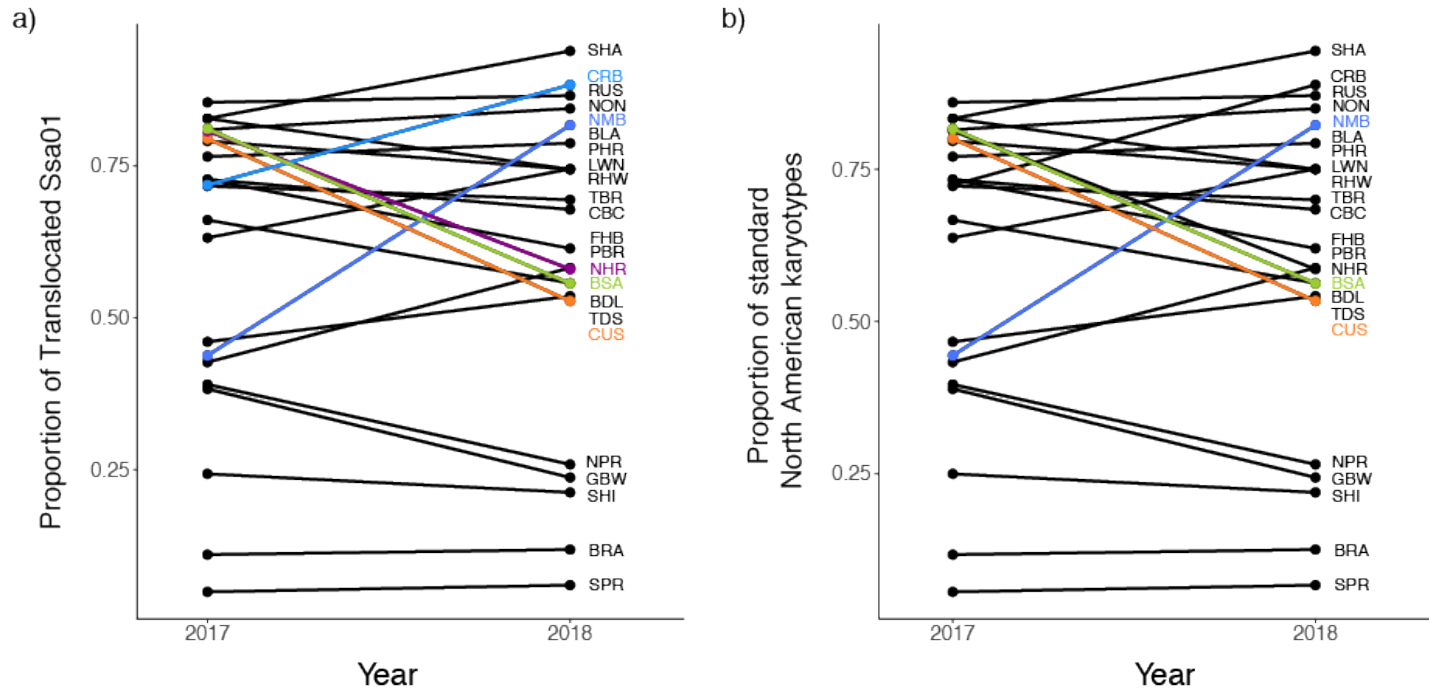
Figure S10 Temporal stability of (a) translocation (b) and karyotype frequencies within river between years sampled (2017 and 2018). Rivers that exhibited a significant change in translocation or karyotype frequency between 2017 and 2018 highlighted. See Figure 1 and Table 1 for location details.

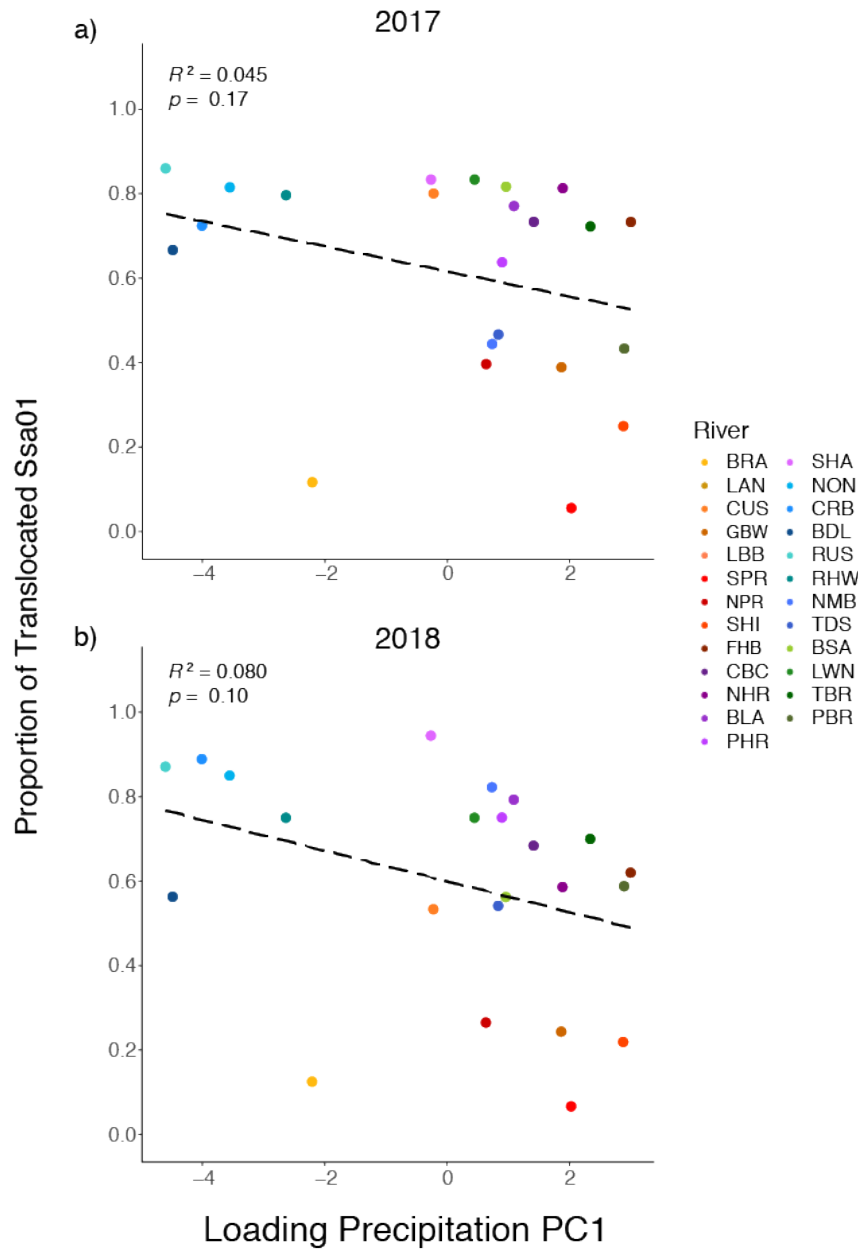Figure S11 Correlation between precipitation and the Ssa01p/Ssa23 chromosomal translocation in Atlantic Salmon within Placentia Bay, Newfoundland, Canada. Linear regression of the first principal component (PC) of a PCA based on 9 precipitation variables (BIOCLIM) and proportion of non-translocated Ssa01p/q sampled in (a) 2017 and (b) 2018.